Experimental and Finite Element Investigation of Resistance Spot Welding of Aluminum AA 2017

JIMMA UNIVERSITY
JIMMA INSTITUTE OF TECHNOLOGY
SCHOOL OF POSTGRADUATE STUDIES

A Thesis Submitted to the graduate studies of Jimma University in Partial Fulfilment of the Requirement for the Degree of Master of Science in Mechanical Engineering (Manufacturing System Engineering)

By

Tewodros Terefe

ID-No-0286/10

March, 2021.

Jimma, Ethiopia

Experimental and Finite Element Investigation of Resistance Spot Welding of Aluminum AA 2017

Jimma University

Jimma Institute of Technology

School of Postgraduate Studies

A Thesis Submitted to the graduate studies of Jimma University in Partial Fulfilment of the Requirement for the Degree of Master of Science in Mechanical Engineering (Manufacturing System Engineering)

By

Tewdros Terefe

ID-No: 0286/10

Advisor: Dr. Besufekad Negash (Ph.D)

Co Advisor: Mr. Srinivasa R.K. (MSc.)

March, 2021.

Jimma, Ethiopia

Declaration

I hereby declare that this thesis entitled **"Experimental and Finite Element Investigation of Resistance Spot Welding of Aluminum AA 2017"** is composed by myself, with the supervision of Dr. Besufekad Negash and Mr. Srinivasa R. K., that the research presented here is my own except where clearly indicated such in the document, and that work has not been submitted for any degree or formal certification in whole or in part.

Student Name:	Tewodros Terefe	Signature: …….	Date: ……..

This research submitted for examination with my approval as the university supervisor.

Advisor:	Dr. Besufekad Negash	Signature: ……	Date: ……..
Co-Advisor:	Mr. Srinivas R. K. (MSc.)	Signature: …….	Date: ……..
Chairperson:	Mrs. Hana Beyene (MSc.)	Signature: …….	Date: ……..

APPROVAL SHEET

JIMMA UNIVERSITY

JIMMA INSTITUTE OF TECHNOLOGY

FACULTY OF MECHANICAL ENGINEERING

This is to certify that the thesis prepared by Tewodros Terefe Adnew, in titled **"Experimental and Finite Element Investigation of Resistance Spot Welding of Aluminum AA 2017"** and submitted in partial fulfilment of the requirement for the degree of master of Science in Mechanical Engineering (Manufacturing System Engineering) complies with the regulation of the university and meets the accepted standards with respect to the originality and quality.

Approved by the examining committee:

Besufekad Negash (Ph.D.)		02/04/2021
Name of Advisor	Signature	Date
Mr. Srinivas R. K. (MSc.)		
Name of Co-Advisor	Signature	Date
Mrs. Hana Beyene (MSc.)		
Name of Chairperson	Signature	Date
Johnson Santosh (Ph.D.)		
Name of Internal Examiner	Signature	Date
Desalegn Wogaso. (Ph.D.)		01-04-2021
Name of External Examiner	Signature	Date

Acknowledgment

First of all, massive thanks to almighty God, for his countless help to complete my thesis successfully.

I would like to express my heart felt appreciation and gratitude to my Advisor Dr. Besufkad Negash and my co advisor Mr. Sernivas K. for their helpful advice and guidance, that they gave to me during my research work to be completed.

I would also like to thank them for giving me valuable support with my research work and run with it which allowed me to proceed the research that much more. Without these ideas, this research paper would not have been the success that it has become and they initiate me for completion of the research.

A special thank goes to Jimma Institute of Technology Staffs and Class mates and who gave me a lot of help through giving strong comments during my writing of thesis.

I would like to thank my entire friends who have contributed to my education and have supported me through my graduate study.

Abstract

Resistance spot welding is a process in which contacting metal surfaces are joined by the pressure and heat obtained from resistance to electric current flow. It is widely accepted in the industry due to its advantages in high speed and suitability for automation. The target is to investigate mechanical properties of RSW, optimize, enhance strength of fabricated by RSW of aluminum**,** by optimizing welding parameters like time, shape of electrodes and sheet thickness of the spot-welded joints finally the checking the micro hardness of the weld structure. In addition, the RSW process is a complicated process that includes electrical, thermal and mechanical phenomena. Percentage contributions of the thickness of aluminum, thickness of cover sheet, and a welding time are 3.89%, 3.25%, and 84.39% respectively. It is found that the degree of importance of process parameters in attaining the tensile strength of weld joint greatly depends on the welding time. In the case of deformation, the percentage of contributions of the thickness of aluminum, thickness of cover sheet, and welding time is 1.17%, 8.73%, and 80.88% respectively. A welding time have the most significant factor. In the case of temperature, the percentage of contributions of the thickness of aluminum, thickness of cover sheet, and welding time is 9.96%, 87.82%, and 1.66% respectively. A thickness of cover mild steel sheet has the most significant factor. Validated result of two selected most significant factors (weld temperature and weld time) validation shows for FEA and Experimental works shows good agreement at weld temperature response, with maximum error of 10.62% that due to nature of the material and influence of other welding parameters such as welding current, thickness of weld cover and welding voltage and thickness of weld itself., as shown the micro hardness test result for the given test specimens HAZ and NZ is various from one region to another. But still it needs further works by changing some weld parameters of the study to know what will happen around the weld zone of RSW.

Key words: *Multi objective optimization, Resistance spot welding, Weld temperature, Weld current, Weld time.*

Contents

List of Abbreviations and Symbols

AA- 2017	Aluminum Alloy 2017
ANOVA	Analysis of variance
AT	Aluminum sheet thickens
ASM	American Standard of Material
CT	Thickness of the cover mild steel sheet
DOE	Design of Experiment
FE	Finite Element
FEA	Finite Element Analysis
FEM	Finite Element Method
FZ	Fusion Zone
HAZ	Heat Affected Zone
IGES	Initial Graphics Exchange Specification
MCDM	Multi-Criteria Decision-Making
MPI	Multi response performance index
NZ	Nugget Zone
RSW	Resistance spot welding
SN	Signal to Noise
UTM	Universal Testing Machine
Wt	Indicates welding time in second

Lists of Table

Lists of Figure

CHAPTER ONE

1. Introduction

Resistance welding is a widely applied joining technique. In this chapter a brief introduction is given to the resistance welding technology. A spot weld is made by pressing two or more pieces of overlapping metal sheets together while an electrical current is passed through a localized contact area to heat the metal to the welding temperature and form the weld nugget. Size and shape of electrodes are critical in spot welding because all the welding current is concentrated in the electrode tip.

1.1. Background

Resistance spot welding is a widely used sheet metal joining process in various manufacturing industries. RSW is processes that produce heat required for welding through what is known as joule ($\boldsymbol{J = I^2Rt}$) heating. Much in the way a piece of wire heats up when current is passed through it, a resistance spot weld forms due to the resistance heating that occurs when current passes through the parts (or sheets) being welded. It is a simple process in which, high current is made to pass through the work sheets under pressure to make the joint. Welding current, welding time and electrode force are the major input parameters affecting the growth of a spot weld. RSW is the most widely used type of all the resistance welding processes. Both electric current and mechanical force are applied simultaneously to make joints in this process. Force is applied to the electrodes to ensure enough contact between the parts to be welded. The welding current and force are applied to the work piece via copper alloy electrodes. The volume of the metal from the work pieces that have undergone heating, melting, fusion and re solidification is called the weld nugget. RSW process is simpler, faster and cheaper compared with most of the other welding processes. RSW can be used to weld several different materials including stainless steel, high strength low alloy steel, advanced high strength steel and low carbon steel, (H. Zhigang et al, 2007, J. Saleem, et al, 2012).

- **Resistance Welding**

Resistance welding is a welding technology widely used in manufacturing industry for joining metal sheets and components. The weld is made by conducting a strong current through the metal

combination to heat up and finally melt the metals at localized points predetermined by the design of the electrodes and/or the workpieces to be welded. A force is always applied before, during and after the application of current to confine the contact area at the weld interfaces and, in some applications, to forge the workpieces. Resistance welding is conducted as follows: Apply force and current through electrodes contacted metal parts to be welded; and resistance heat is generated at the interface of metal parts and makes a nugget, resulting in melt joint. Though a large current flow, there is no danger of an electric shock because only low voltage is impressed, (Alden, 2017).

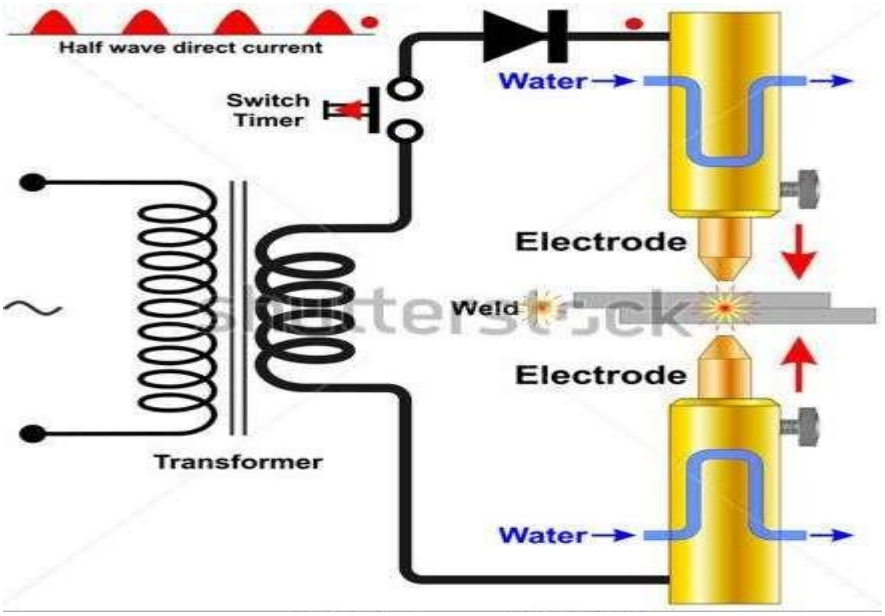

Figure 1.1. Resistance spot welding circuit (Raut & Achwal, 2014)

- **Welding Parameters**

The quality of a weld joint welded by RSW largely depends on the input process parameters. The spot-welding process includes several variables that can be adjusted to achieve optimum welding performance. (Alden, 2017, Gery D. et al. 2005 and Joo B., et al, 2005**)**

The welding current is the current that flows through the work piece. Of all the parameters, it is this that has the greatest effect on strength and quality of the weld, as the amount of heat produced is proportional to the square of the welding current. The welding current must therefore be carefully adjusted: too high a current result in a weld with poor strength, with too great a crater depression, spatter and some distortion. It also means that the electrodes are worn unnecessarily.

Too low a current, on the other hand, also produces a weld of limited strength, but this time with too small a weld area, (Alden, 2017 and O. Andersson, 2013).

Squeeze time is the time needed to build up the clamping force. It varies with the thickness of the metal and with the closeness of the fit, and is also affected by the design of the electrode jaws. The clamping force is the force (KN) with which the electrodes press the sheets together. It is important that this should be carefully controlled, as too low a clamping force results in a high contact resistance, accompanied by spatter and resulting in a poor weld strength while too high a force results in too small a weld, again with poor strength, but accompanied by unnecessary wear on the electrodes and too great a crater depression, (Alden, 2017).

Welding time is the time for which current flows through the work piece, and is measured in cycles, i.e. during which alternating current passes through one cycle. In Europe, the mains frequency is 50 Hz, which means that one cycle takes 1/50 = 0.02 s. Hold time is the time from when the current is interrupted until the clamping force can be released. The plates must be held together until the weld pool has solidified, so that the joint can be moved or the electrodes moved to the next welding position. The electrode area determines the size of the area through which the welding current passes, i.e. the current density, (Alden, 2017).

- **Electrodes and Electrode Degradation**

The function of alloyed copper RSW electrodes include applying force to the work piece, providing necessary current densities and facilitating post-weld cooling. Typical electrode geometries are shown in Figure 1.2. Truncated electrodes are commonly used in industrial applications due their limited contact tip growth. However, care must be taken during alignment of truncated electrodes since the weld quality can be severely affected with misalignment. Dome type electrodes are less susceptible to misalignment issues and are commonly employed for industrial applications, (Rysul & Shawon, 2014).

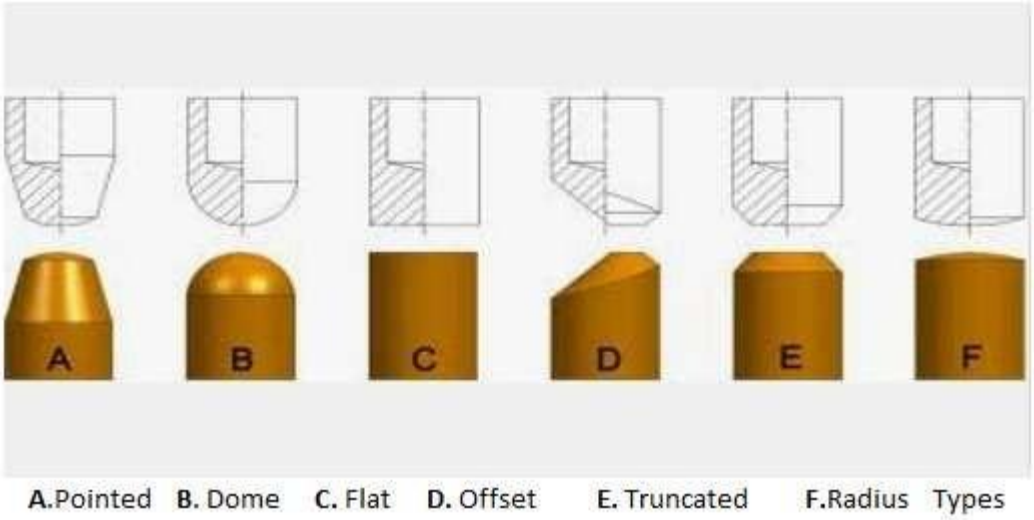

Figure 1.2. Common Electrode Geometries (Rysul & Shawon, 2014)

- **Electrode Materials**

The most important function of the spot-welding electrode is to conduct electric current and to squeeze the sheets together. Therefore, electric conductivity, compressive strength and hardness are important factors in finding an appropriate electrode material. The material that fits the demands best is copper and copper-based alloys, as described in the standard ISO5182:2008. The most common electrode material is a copper-chromium zirconium alloy, while higher resistance alloys of nickel, beryllium and/or cobalt may be used for higher strength steels and stainless steels (Lai and G. L, 2010).

- **Finite Element Modeling of RSW**.

Finite Element Analysis (FEA) of the digital computer enables effective problem solving and complex problems in structural dynamics. Structural dynamics can be solved in the frequency domain using the transformation of the modal. Finite element code efficiently performs structural dynamics response calculations involving harmonic response, transient response and random structure of the complex. Therefore, the finite element method offers a highly efficient procedure for the calculation of complex linear structure under dynamics excitation conditions variables.

The Finite element method is a procedure to numerically find approximate solutions to partial differential equations for a system representing a real-world problem. The system is divided into elements to better represent various material properties in the domain. Several Finite Element

models have been developed to replace the physical verification of RSW. This is due to the high costs and time consuming of the physical testing and to obtain better understanding of the process. To create an accurate Finite Element model of RSW coupling between the mechanical, thermal and electrical models are required (O.P Gupta and Amitava De, 1998 and H.A Nied, 1984).

Most of the finite element computer programs are very large in size and it requires larger computer with large memories in which to operate. Hence, it is very costly for the companies to invest large amounts of money to develop a single finite element model. In additions, the model are time consuming to create and verify, it can be sensitive to boundary conditions and sometimes model needs to be refined regularly to give assurance that the results are reasonably accurate (Alden, 2017).

1.2. Statements of the Problem

Now a days, Aluminum is more applications in automotive industry, especially for body paneling of railcars. RSW is a prominent welding process in this area. Due to difficult nature of aluminum the welding is not easy task as welding of steel, even though aluminum is very essential material in modern light weight applications for example the most car bodies were made of through resistance spot welding of aluminum alloys, but still not AA2017 families. Besides to this, metals better conductors of electricity such as aluminum are more difficult resistance welded than higher resistivity such as steel which are more easily resistance welded. Quality and performance characteristics of resistance spot welds are essential for the safety design of the vehicle.

It should, however, be emphasized that RSW of aluminum is more problematic than steel due to higher electrical and thermal conductivity, higher coefficient of expansion, lower melting temperature, and an oxide layer, which has high electrical resistance and high melting temperature (2050 °C).

There are a couple of characteristics of aluminum that make it more difficult to resistance weld than steel. The most significant is its high electrical conductivity, requiring high welding currents and large capacity equipment, (Gery D. et al. 2005**,** Moarref zadeh, 2011 and Lai and G. L, 2010). Secondly, the electrodes are made from copper which alloys with aluminum, resulting in rapid wear and a short electrode life.

As with conventional fusion welding, resistance welding suffers from similar problems of oxide entrapment and hot cracking, the latter not being helped by the lack of a more crack-resistant filler metal, and porosity, (Moarrefzadeh, 2011 and Lai and G. L, 2010).

1.3. Objectives of the Research

1.3.1. General Objective

The primary objective of this research is to perform experimental and finite element investigation of resistance spot welding on aluminum AA 2017.

1.3.2. Specific Objectives

- To investigate the mechanical properties of resistance spot welded joints of aluminum alloy 2017.
- To optimize the welding process parameter of resistance spot welding.
- To investigate the optimized welding process parameters on the output by using design of experiment.

1.4. Significance of the Research

Resistance spot welding (RSW) is vastly used in automobile industries to cut weight and lower the cost. The aim of this research is to find out the effect of spot weld parameters on the strength of spot weld. The effect factors of multiple spot-welded joints strength are analyzed including, surface microstructure of welded area, hardness of welded area spot weld diameter and thickness based on finite element analysis (FEA) and experimental results on aluminum alloy 2017. The research result shows that weld diameter and thickness are primary factors affecting the strength of the joints for a given material. Based on effect factor analysis the optimized parameters are also discussed to improve the strength of structure.

1.5. Scope of Study

Mechanical properties of resistance spot-welded joints of aluminum alloy AA- 2017 sheets are investigated in this study, with the focus mainly on its weld joint strength and optimization using Taguchi approach.

1.6. Limitation of the Study

This research addressed experimental and finite element investigation of resistance spot welding on aluminum AA 2017, for a limited electrode force, electric voltage, electric current, and much focused on addressing the research objectives mentioned on section 1.3 of this chapter which were investigation on the hardness of weld area, identifying the mechanical property of the weld area and optimization, due to certain constraints the study was limited so that the paper was limited to answer all RSW related questions for exam identifying weld zone nugget size and others.

1.7. Organization of Thesis

This thesis report consists of five chapters each of the chapters are focuses on the Experimental and Finite Element Investigation of Resistance Spot Welding on Aluminum AA-2017. This thesis paper comprises of following basic points in each chapter.

Chapter 1: - Introduces the background of resistance spot welding, spot welding parameters and the main factors that should considered while welding of soft metals and this research Statement of problem, objectives, significance of the study, Scope of the study is discussed.

Chapter 2: - Reviewed all relevant research papers regarding spot welding, steel and aluminum materials weld cycles, welding current, welding time, electrode cup diameter, electrode force significance on resistance spot welding is discussed and presented by other scholars were discussed clearly and identified the literature gap with this thesis work widely and deeply reviewed.

Chapter 3: - Material and methods used during the research work is studied and the steps used for conducting the experiment and FEA steps are putted clearly.

Chapter 4: - The result and discussion of the experimental and FEM work is shown and discussed briefly. Finally optimization is done based on the three identified and selected parameters, to reduce cost of experiment only three test samples were taken then micro hardness tests were done by using multi objective optimization and

Chapter 5: - According to the result obtained in the above chapter's conclusion and recommendation were made, finally the future working areas are put as the directions.

CHAPTER TWO

2. Literature Review

2.1. Introduction

Resistance spot welding (RSW) is a proficient joining method commonly used for sheet metal joining. RSW has outstanding technical and economic advantages, such as its high speed, suitability for automation and low cost, which make it an attractive choice for the production of auto bodies, truck and rail cabins, home appliances etc.

Resistance spot welding (RSW) is the most dominant process in sheet metal joining, particularly in automotive industry due to low cost, high productivity, flexibility, easy automation and maintenance, and minimum requirements for skilled labor. The process is also widely applied in other industries of sheet product manufacturing, e.g. other transportation industries and in production of kitchen utensils. It should, however, be emphasized that RSW of aluminum is more problematic than steel due to higher electrical and thermal conductivity, higher coefficient of expansion, lower melting temperature, and an oxide layer, which has high electrical resistance and high melting temperature (2050 °C). The latter together with the fact that the effective contact resistance grows considerably as the oxide film grows implies large scatter in quality of RSW aluminum sheets, which therefore require close production control. The high thermal and electrical conductivity of aluminum require 2–3 times higher current and shorter weld time, typically 25% of that used to spot weld steel. Accurate control and synchronization of current and electrode force is required due to the narrow weld temperature range. The problems are especially pronounced when welding unalloyed aluminum (Naimi et al., 2015).

2.1.1. Spot Welding

Resistance spot welding is one of the oldest electric welding processes in use by industry today, especially in the automotive industry. Welds made by a combination of heat, pressure, and time. As the name resistance welding implies, it is the resistance of the material to be welded to current flow causes localized heating in parts. The pressure exerted by the tongs and electrode tips, in which the current flows, holds the parts to be welded in intimate relationships before, during, and after the welding cycle.

The amount needed during the course of time in the joint is determined by the thickness and type of material, the total running time, and the cross-sectional area of the surface of the welding contact tip, figure 2.1 show the spot-welding process: (Handbook for Resistance Spot Welding 2012).

2.1.2. Mechanism of Resistance Spot Welding

Resistance Spot Welding (RSW) is included in the group of resistance welding processes that heat is used in joining the work parts of metal. Heat is generated from electrical resistance across the two work parts in Resistance Spot Welding two work part of metal are joined together by applying electric current and pressure in the zone to be weld and resistance welding is different from arc welding because it's not required filler metal or fluxes added to the weld area during the welding process (Alden, 2017).

Spot welding operates based on four factors that are:

- **i.** Amount of current that passes through the work piece.
- **ii.** Pressure that the electrodes applied on the work piece.
- **iii.** The time the current flow through the work piece.
- **iv.** Area of the electrode tip contact with the work piece

In the spot-welding process, two or three overlapped or stacked stamped components are welded together because of the heat created by electrical resistance. This is provided by the work pieces as they are weld together under pressure between two electrodes. Spot welding may be performed manually, robotically or by a dedicated spot-welding machine. The similar spot welds having same property can be obtained in high production speeds by controlling welding current, electrode force and weld time automatically, figure 2.1 and figure 2.2,show the cycle of spot weld (Alden, 2017).

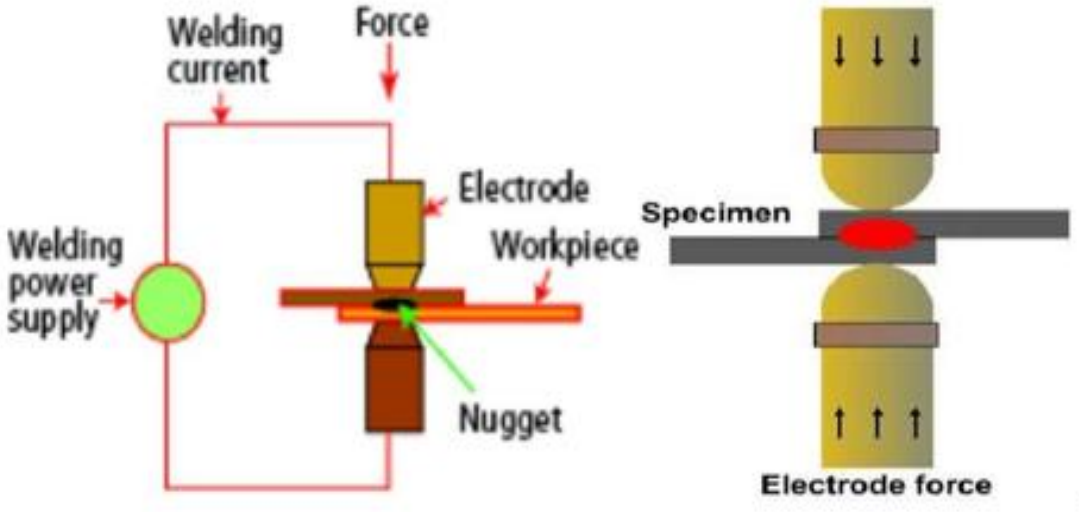

Figure 2.1.Schematic view of the spot-welding process (Alden, 2017)

2.1.3. Principles of Spot Welding

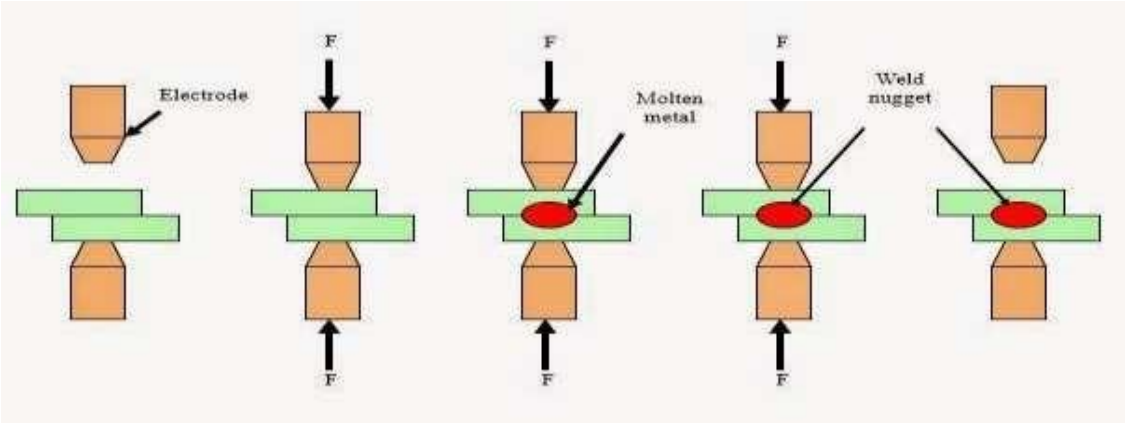

Figure 2.2. Cycle of Spot Welding (Alden, 2017)

The processes in resistance spot welding have 5 cycle process as shown in the Figure 2.2.

The first cycle is the squeeze time, where pressure from the electrode force is applied to the work piece. The second cycle is weld time, this process where the current is on and the welding current is applied in the metal sheets to melt the sheet metal for the welding process. Then, post heat time, the current delay at the low level. The fourth cycle is cool time. This cycle allows the melt nugget diameter to solidify before the releasing the welded parts and lastly the off-time cycle, the electrode force applied on the sheets metal is released the welding process is done.

There are six major points of resistance in the work area. They are as follows:

i. The contact point between the electrode and top work piece.
ii. The top work pieces.
iii. The interface of the top and bottom work pieces.
iv. The bottom work piece.
v. The contact point between the bottom work piece and the electrode.
vi. Resistance of electrode tips.

2.2. Materials welded by Resistance spot welding

2.2.1. Steel

The performance of resistance spot-welded joints in advanced high-strength steel sheets is critical for the application of these materials in safety-critical areas. To be able to predict the performance of such joints from available material data would be of great benefit to the automotive industry. A set of resistance spot-welded joints in various advanced high-strength steels was tested with lap shear and peel-type tensile testing. Testing was done both statically and dynamically. The steel sheet materials varied in microstructural and chemical compositions, strength and thickness. The weld process settings were defined so that all welds would have a weld nugget size of approximately $4\sqrt{t}$, with the sheet metal thickness (K. Kim, 2000).

In lap shear tensile tests (static and dynamic), welds pre- dominantly failed interracially. In peel type tensile tests, welds failed predominantly in pull-out failure modes. It was found that an increase in the strength of the joints in static testing corresponds with an increase in strength in dynamic testing. This was true for both lap shear and peel-type tensile testing.

The only straightforward relation between the material characteristics and the performance of the joints that could be derived from the results reported here was an increase in strength with an increase in sheet metal thickness. It is thought that this corresponds with an increase in weld nugget size (as the size of the weld nugget is dependent on the sheet thickness).

No relation could be derived from these results between the tensile strength of the welded joints and mechanical characteristics of the sheet metal. This does not imply that there is no such relation for subsets of materials (e.g. of similar thickness). Such a relationship is even likely, but it could not be derived from the wide set of material characteristics as used for the experimental work for this report.

Post weld hardness is often blamed for issues with the performance of advanced high-strength steels, and credited for their strength. However, no strong relation could be found between the carbon content of the base metal and the performance of the welded joints. Neither could a relationship be found with various carbon equivalent numbers linking the chemical composition of the material with its hardenability. Again, this does not imply there is no such relation for subsets of materials (e.g. of similar thickness), as such a relationship is highly likely, but it could not be derived from the wide set of material characteristics as used for the experimental work for this report. The performance of resistance spot-welded joints in advanced high-strength steel sheets can probably not be linked with a single material characteristic. When such claims are made, the experimental conditions should be clearly identified. In this work, for instance, a relationship could be derived between sheet metal thickness and tensile strength of the spot-welded joint, but this was very likely closely related to the fact that the weld process set- tings were defined so that all welds would have a weld nugget size of approximately $4\sqrt{t}$, [Den Uijl et al., 2012].

The damage sequence of AHSS spot welds in cross tension was characterized in this study by means of coupled micro tomographic, metallographic and fractographic analyses. Three main failure mechanisms and failure zones were identified strain localization in the BM/SCHAZ, (ii) ductile shear around the weld from the notch tip and (iii) semi-brittle fracture in the weld nugget, starting at the faying surface. The final failure type and load bearing capacity of a spot weld results from a competition between these main failure mechanisms, which may take place simultaneously, giving rise to a wide variety of spot weld fracture appearances. Next, a FE model of spot weld behavior was developed in order to illustrate the competing mechanisms leading to a given failure type. The local constitutive behavior was obtained by tensile testing simulated spot weld HAZ microstructures and the resulting ultimate fracture strains were used as local failure criteria. This allowed reproducing the main trends in the ductile fracture of spot welds, i.e. the transitions in failure type and a relevant estimation of the load bearing capacity, [Dancette et al., 2011]

2.2.2. Stainless steel

Austenitic stainless steels are widely utilized in industrial applications due to their strength, corrosion resistance, mechanical workability, and excellent electrical and thermal conductivities. Among them, ASS 316 stainless steel is of great practical interest because it is employed in pharmaceutical, petrochemical, offshore drilling marine shipping, water desalination, etc. Weld current is major governing factor affecting the tensile shear strength of the resistance spot welded

specimens. As the weld current increases, size of weld nugget also increases. This results into increased values of tensile-shearing strength, (Shelly & Sahota, 2017).

Understanding phase transformations during RSW of stainless steels is a key in understanding of mechanical behavior of the weldment. In this paper, the micro- structure evolution mechanism of the HAZ of the stainless steels of austenitic, ferritic and DSSs during RSW are examined and analyzed. The following conclusions can be drawn from this work: -

i. The ASS exhibited grain growth in HAZ producing a soft region compared to the BM which served as a preferred fracture path during PF of the welds.

ii. The grain growth and martensitic formation were main metallurgical features of the HAZ of FSS. The HTHAZ exhibited almost martensitic free ferritic microstructure with excessive grain coarsening due to the absence of the elevated temperature austenite to pin the grain boundaries. The LTHAZ, which exhibited the highest hardness in the HAZ of FSS, shows ferrite martensitic dual phase microstructure with limited grain growth. The BM remained the softest region in the weldment, which served as a preferred fracture path during PF of the welds.

iii. The ferrite/austenite unbalance was the main feature of the HAZ of the DSS. It was affected by both the presence of Tic C in the initial microstructure of DSS and rapid cooling rate of RSW process. In the HTHAZ, which exhibited the highest hardness in the weldment, the dissolution of Tic C increases the carbon content of the d-ferrite and hence promotes the austenite reformation during d_{Rc} transformation. In LTHAZ, which exhibited some degree of softening, rapid cooling rate suppresses the solid-state ferrite–austenite transformation during cooling producing high d/c ratio

iv. For all investigated steels, the FZ size at sheet/ sheet interface is the key macrostructural feature controlling the load bearing capacity and energy absorption capability of spot welds. It was shown that there is no correlation between tensile strength of the BM and mechanical properties of the welds. The hardness characteristics and failure mode of the welds affect the mechanical properties of the joints, [Alizadeh-Sh et al., 2015].

2.2.3. Dissimilar Material

As per the research finding by (H. Zhigang, 2006) the following points are key factors in RSW.

- The thickness results an increasing in shear force of spot welding.
- The center of nugget zone has the maximum value of hardness.
- This decrease gradually through the HAZ.
- The maximum shear force (1.14 KN) has been optimized to reach the value (1.24 KN) by apply DOE with using welding parameters welding current (13600A), electrode force (1.6 KN), squeeze time (30 c) and welding time (25 c).
- Due to heat generated, very fine equated grains and uniformly distributed fine precipitates were observed in the NZ of AA 6061-T6.
- A mixture of ferrite and bainite is observed in the NZ and HAZ of AISI 1010. 6.
- The nugget diameter is increased when the electrical and thermal coefficients decrease, at the same time the HAZ is decreased when the electrical and thermal coefficients increase.

2.2.4. Aluminum

Based on the experimental work reported above, it is evident that the surface condition of the sheet material produced through different manufacturing processes has a significant effect on the RSW process, electrode condition and weld quality.

a) For RSW structural applications; an incomplete removal of 'disrupted surface layer' prior to surface pretreatment has a detrimental effect on the RSW process. Therefore, 'full clean' manufacturing process is recommended to avoid the occurrence of sticking and to maintain the electrode condition. This should also ensure a consistent process window that is essential for a manufacturing situation.

b) Removing the wax lubricant reduces the static contact resistance, but in practice lubricant is a necessary component of the overall process. Therefore, a weld schedule with a low current pre-pulse, made prior to the main weld can be used to displace the lubricant and normalize the surface reducing the risk of expulsion.

c) For RSW closure applications; AA6111T4 with either MF or EDT surface have acceptable spot-welding process windows. The use of an EDT surface has been shown here to extend the useable welding range.

d) Close participation between materials suppliers and automotive manufacturing Centre's is required to ensure optimum process parameters are applied at all stages of manufacturing for specific applications, (Lövenborn, 2016).

The objective of this research was to investigate whether spot welding between aluminum and steel can be achieved using a transition material. Experimental approaches were used in determining the optimal electrode combinations and welding parameters. Nugget formation process was then examined using consecutive metallurgical cross-sectioning. It was found that two distinct fusion zones formed during the spot-welding process of aluminum to steel using a transition aluminum-clad steel strip. The nugget on the steel side is a regular, elliptical weld with dendritic grain structure inside the nugget region. The nugget on the aluminum side is the top half of the elliptical shape. Also, a thin, inter metallic compound formed on the aluminum/steel clad interface due to the welding heat input. Static, dynamic, and fatigue performances of these welds were then examined and compared with the self-piercing rivet population of the same dissimilar materials combination. It was found that the static and dynamic strength of the RSW samples are comparable to those of the strength of the self-piercing rivets under the same loading conditions.

However, because of different failure modes, the lap shear dissimilar RSW samples have a considerably lower energy absorption level than the dissimilar SPR samples. Fatigue strength comparison of the RSW population and the SPR population indicates that SPR population has much higher fatigue resistance than the spot welds. This study demonstrated the spot weldability of aluminum to steel with transition clad material and evaluated the structural performance of these welds. The corrosion related performance evaluation for the dissimilar RSW population is currently being pursued. It should be mentioned that the cladding ratio of the transition material used in this study was not optimized. With an optimized cladding ratio, it is conceivable that the weld static strength, failure mode, and energy absorption of the dissimilar RSW population can be further improved. It should also be noted that the economic and production feasibilities of introducing such transition welds into automotive production need to be further studied and justified. First of all, spot welding using the transition material adds weight to the entire vehicle. Secondly, the relatively low yield of the cladding process would translate to the potential material cost increase for the automotive industry. Furthermore, the difference in thermal expansion coefficients of the two cladding materials would promote thermal distortion of the parts made of these materials.

Nonetheless, the results of this study do suggest the potential application of aluminum clad steel as a load-bearing structural component as well as a material transition between the possible aluminum parts to the steel parts of the vehicle for optimized safety and weight reduction of a particular vehicle design, [Sun & Khaleel, 2004].

2.3. Process Model

The large number of parameters involved shows how complicated a process resistance welding is. To evaluate a resistance welding process, one must consider all the factors as a whole, see figure 2.3.

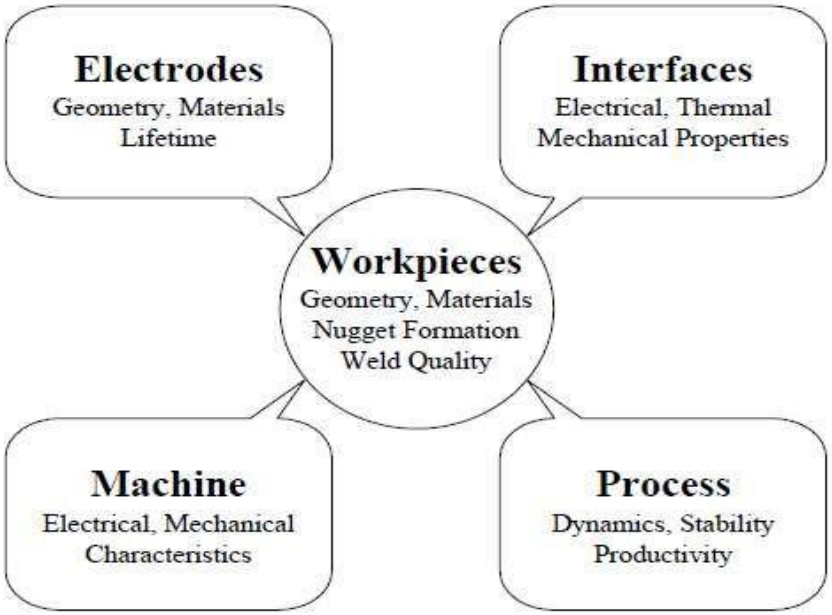

Figure 2.3. The system of parameters in resistance welding [Wenqi Zhang, 2000].

2.3.1 Numerical

- The contact radius of the electrode/sheet contact surfaces is basically equal to the electrode radius in the preloading stages, while the value of sheet/sheet contact surface is much larger.
- The formation of the nugget in theoretical analysis undergoes three stages: plasticity adhesion, rapid growth, and slow growth.

- Close correlation is observed between simulated thermal fields and the microstructure changes of joints. The longer the dwell time temperature is larger than the austenitic initialization of the joints, the coarser the martensitic that will be generated.
- It should be pointed out that the error is about 10% as the welding current is very large and the expulsion occurs. When the expulsion occurs, molten metal splashes from the welding zone and the nugget size is smaller than expected, however, this can't be considered in the finite element modeling.
- The accuracy of the physical experiments and numerical simulations is within the acceptable range. It is a real potential for the simulated results to be adopted by a wide range of users for process planning in modern manufacturing, [Zhao et al., 2019].

2.3.2 Analytical

For the first time, an analytical model of the heat conduction in the small-scale resistance spot welding process was developed and analyzed. Solutions to a one-dimensional model and an axisymmetric two-dimensional model of the process were obtained using superposition and separation of variables. Temperature fields and temperature histories were calculated. The feasibility of real-time implementation of the model is discussed and the potential of the two-dimensional model to handle an arbitrary current distribution is demonstrated. To refine the model for more accuracy to serve as the basis for a real-time control, it is believed that further work is needed. A mechanical–electrical contact analysis of the faying surface between the metal sheets would be preferred to provide an estimate of current density distribution across the faying interface. Since the computational demands of the thermal model seem to be within the capability of current DSP chips, the addition of a thermal–mechanical analysis is also planned. This will allow the analytical model to predict the thermal expansion of the work, and thus electrode displacement, during welding. This prediction can then be compared to real time measurement to provide information about the nugget development and real-time corrections of the model for more accurate nugget thickness predictions, [Chen & Farson, 2006].

2.4. Advantage of Resistance Spot Welding

The major advantages of resistance spot welding are its high speed and adaptability for automation in the high-rate production of sheet metal assemblies. Spot welding is also economical in many job

shop operations because it is faster than arc welding or brazing and requires less skill to perform, [Brien, N.2000].

As stated above, aluminum is an essential material that makes working easy in construction and marine industries, its alloys, on the other hand, are also crucial. One of the most famous and used aluminum alloys in the market is Aluminum 2017 alloys. In general, all the aluminum 2017 alloys that got molded into sheets and plates are heat treatable wrought material with intermediate strength capacity.

- Storage Tanks, -Train
- Spacecraft Fuel Tanks, -Aerospace
- Boat Floor, - Automobile Bodies
- Home Appliances

2.5. Application of Resistance Spot Welding

Resistance spot welding is used to fabricate sheet metal assemblies up to about 3.2 mm (0.125 in.) in thickness when the design permits the use of lap joints and leak-tight seams are not required. Occasionally the process is used to join steel plates 6.35 mm (1/4 in.) or more in thickness; however, the loading of such joints is limited and the joint overlap adds weight and cost to the assembly when compared to the cost of an arc welded Stainless steel, aluminum, and copper alloys are commonly used metals in commercial spot welding. The process is used extensively for joining low-carbon steel sheet metal components for automobiles, cabinets, furniture, and similar products. Resistance spot welding is used in preference to mechanical fastening, such as riveting or screwing, when disassembly for maintenance is not required. It is much faster and more economical because separate fasteners and additional filler materials are not needed for assembly, (Brien, N.2000).

2.6. Effects of Resistance Spot Welding on Aluminum Alloy

The chemical affinity of aluminum for oxygen causes the aluminum to become coated with a thin film of oxide when it is exposed to air. The thin oxide film that forms on a freshly cleaned aluminum surface does not cause sufficient resistance to be troublesome for resistance welding. The permissible holding period, or elapsed time between cleaning and welding, may vary from 8

hours to 48 hours or more, depending on the cleaning process used, the cleanliness of the shop, the alloy, and the application.

Based on the experimental work reported above, it is evident that the surface condition of the sheet material produced through different manufacturing processes has a significant effect on the RSW process, electrode condition and weld quality.

a) For RSW structural applications; an incomplete removal of 'disrupted surface layer' prior to surface pretreatment has a detrimental effect on the RSW process. Therefore, 'full clean' manufacturing process is recommended to avoid the occurrence of sticking and to maintain the electrode condition. This should also ensure a consistent process window that is essential for a manufacturing situation.

b) Removing the wax lubricant reduces the static contact resistance, but in practice lubricant is a necessary component of the overall process. Therefore, a weld schedule with a low current pre-pulse, made prior to the main weld can be used to displace the lubricant and normalize the surface reducing the risk of expulsion.

c) For RSW closure applications; AA6111T4 with either MF or EDT surface have acceptable spot-welding process windows. The use of an EDT surface has been shown here to extend the useable welding range.

d) Close participation between materials suppliers and automotive manufacturing Centre's is required to ensure optimum process parameters are applied at all stages of manufacturing for specific applications, (Han et al., 2010).

Taguchi methods is a statistical approach developed to enhance the quality of manufactured goods and more recently it is applied to engineering, biotechnology, marketing and advertising also. In most quality control situations, the goal is to produce output as uniformly near a target value as possible and the reduction of variation is now regarded. These three are: large values are better, smaller values are better, target values are better. Taguchi method employs a systematic approach to the robust design by increasing performance quality and decreasing the cost. Two major tools used to optimize the process parameter are signal to noise ratio and orthogonal array (Jana N. et al. 2009 and Vikas P. et al. 2013).

2.7. Major Research Gap Identified

As reviewed on the above relevant literatures, the following research gaps are observed: -

For RSW structural applications; an incomplete removal of 'disrupted surface layer' prior to surface pretreatment has a detrimental effect on the RSW process. Therefore, 'full clean' manufacturing process is recommended to avoid the occurrence of sticking and to maintain the electrode condition. This should also ensure a consistent process window that is essential for a manufacturing situation.

- No paper was done on AA2017 family of aluminum.
- No study result was captured with such small electric current and voltage.
- As per knowledge on RSW there was no clear understanding what was going on behind the experimental scenario so to know that and put basic scientific footstep for future researchers the study done on new family of aluminum. On the other hand:-

Therefore, a weld schedule with a low current repulse, made prior to the main weld can be used to displace the lubricant and normalize the surface reducing the risk of expulsion. This application of control method of current gain compensation of new current step, the abrasion of electrode cap diameter is kept within 1.5mm and the current density is about greater than 275A/mm^2. It meets requirements of acquired acceptable welding spots and such electrode cap can be used after polishing.

CHAPTER THREE

3. Material and Method

3.1. Detail of Experiments and Simulations Procedures

This chapter will discuss flow of the research. The purpose of this research is to study the mechanical properties of aluminum alloy AA 2017 joint by using the cover layer of Mild Steel 1010 produced by Resistance Spot Welding (RSW). Parameters that had been used for this welding technique are different thickness of aluminum sheet, different thickness of mild steel sheet, and welding time. Dynamic properties of this materials joint can be determine using experimental investigation and numerical analysis through ANSYS (FEA). Finite Element Analysis results will be compared and validate with Experimental investigation results.

3.1.1. Selection of Material

In order to obtain a good quality result of (RSW) joint, a proper selection of materials is important because of its mechanical properties of material and material composition. Aluminum alloy AA 2017 is the series of the most widely being used structural materials in automotive, aerospace industries and rail transportation. Therefore, aluminum alloy 2017 had been chosen for this research.

- Study on Mechanical Properties of aluminum alloy AA 2017

Aluminum/aluminum 2017 alloy is a heat treatable wrought alloy with intermediate strength. It is stronger than aluminum /aluminum 2011, but harder to machine. Workability is fair with ductility and formability better that aluminum / aluminum 2014.

One of the most essential and crucial chemical elements found in earth's crust for effective working in industries like automobile and construction is aluminum. Aluminum and its alloys are predominant metals typically comprising of elements like zinc, silicon, copper, magnesium, and manganese. By varying the composition different-different products can be formed for industrial usage.

It is much stronger and ductile compared to other grades in the aluminum alloy series. Corrosion resistance is completely fair whereas resistance weldability and arc weldability is satisfactory. The aluminum 2017 plates have low density and appropriate melting point both in metric as well as in imperial see figure 3.1. What makes it so essential in industries? It is yielding strength, shear strength, elongation (annealed), tensile strength (annealed), and elastic modulus. Similar to density and melting point, you can get in metric and imperial units too. Other property that makes it an ideal product is thermal expansion and thermal conductivity. The aluminum alloys exhibit other designated forms also. Know how machinability formability and welding have an impact on it.

3.1.2 Chemical Compositions and mechanical properties of the materials

Figure 3.1. Chemical Compositions of aluminum alloy AA 2017

Table 3.1.Chemical composition of aluminum alloy AA 2017

Al 2017	Al	Si	Fe	Cu	Mn	Mg	Zn	Cr	Ti
Percentage	99.47	0.023	0.409	0.0684	0.0027	0.001	0.005	0.001	0.001

Table 3.2. Mechanical property of aluminum alloy AA 2017

Material	Ultimate tensile strength	Yield strength	Elongation in %
Al 2017	379Mpa	221Mpa	12

➢ **Mechanical properties of Cover material mild steel 4130**

In material selection, carbon steels generally are classified by their proportion (by weight) of carbon content. The low the carbon content, usually called as mild steel, which has less than 0.30 % C. Mild steel basically used for industries as a product, for example bolts, plates and nuts. The 4130 is a code of the American Iron & Steel Institute and defines the approximate chemical composition of the steel. The "41" denotes a low alloy steel containing nominally 1 percent chromium and 0.2 percent molybdenum (hence the nickname "Chromalloy") AISI 4130. Chromalloy steel is actually alloy steel grade 4130. The added chromium and molybdenum help to give the steel different properties from its mild steel counterpart, AISI 1030, even though they have the same percentage of carbon. AISI 4130 is a low alloy steel containing molybdenum and chromium as strengthening agents. The carbon content is nominally 0.30% and with this relatively low carbon content the alloy is excellent from the fusion weld ability standpoint. The alloy can be hardened by heat treatment.

➢ **Application of mild steel 4130**

Summary, 4130 steel alloy is famous for its strength property when it is used for heat treatment. The importance of this steel is in aircraft manufacturing companies and welding purpose. It has features of both chromium and molybdenum steel alloys.

Figure 3.2. Chemical composition of mild steel 4130 sheet for the cover purpose

Table 3.3.Chemical composition of mild steel 4130 sheet for the cover purpose

Percentage	Fe	C	Si	Mn	Cr	Mo	Ni	Co	Cu
Mild steel	99.26	.0349	.400	0.193	0.0305	0.030	0.0152	0.002	0.0346

3.2. Oxford Instruments PMI-MASTER Smart

Oxford Instruments PMI-MASTER Smart meets the latest technical standards and is the first truly portable optical emission spectrometer for metal analysis.

In the figure 3.3 illustrated portable optical emission spectrometer is light weight and small size, the PMI-MASTER Smart can be conveniently carried, making the analysis independent, especially in hard to reach places. Despite its compact dimensions it offers high analysis performance. The rechargeable battery pack provides enough power for approx. 10 h in standby, 300 measurements in spark mode or 200 analyses in arc mode, depending on the measurement conditions. The PMIMASTER Smart can also be operated using the external power supply/charger, with or without battery and even when recharging the battery pack. Due to minimized Argon consumption bottle is sufficient for several analysis. For more intensive use a cart, holding a 10 bottle, is available.

Figure 3.3. Portable optical emission spectrometer for metal analyzer

3.3. Experimental Study on Resistance Spot Welding Machine

3.3.1 Welding Parameter Selections

With the selected electrode combination, optimal welding parameters were determined by iterative welding trials. So many thicknesses of aluminum alloy from the thickness of 0.7 mm and 1.3 mm mild steel cover materials thickness of 0.6mm -1.0 mm were used. Peel and lap-shear tensile tests were used to provide a quick estimate of the weld quality. The results of the peel tests indicated

that a weld button was easily achieved when peeling was conducted between the welded aluminum sheets. However, it was extremely difficult to obtain a consistent full button pullout when peeling was conducted between the welded aluminum sheets, even for the samples made with the same welding parameters. Since the peel test results were inconsistent, lap-shear tensile tests were also used to evaluate the weld quality.

After 36 iterative welding trials, the following welding parameters were finalized for spot welding of 0.7-mm, 1.0-mm and 1.3-mm-thick aluminum alloy AA 2017, and 0.6-mm, 0.8-mm, and 1.0mm of mild steel cover.

- Electrode on both side: tapered flat the tip is prepared.
- Electrode force: asper the machine standard we have fixed electrode force 1.6 KN.
- Welding current 3 kA

3.4. Specifications of Resistance Spot Welding Machine

Figure 3.4. Hand Held Mini Spot-Welding Machine

Table 3.4. Welding Machine Details

Manufacturer	**China -time way**
Type	Hand held resistance spot welding machine
Transformer Capacity	3 KVA
Electrode Force (max)	3 KN
Water Flow Rate	2 litter / min
Cooling	Air
Welding Capacity (sheet metal)	0.5-1.5 mm
Welding current(max)	3000(A)

Phase	Single phase
Throat depth	100mm
Frequency	50Hz +/- 3%

3.5. Sample Preparation

Sample material with thickness 1mm will be cut using shearing machine with dimensions specified for mechanical tests switch on the machine, make sure the hydraulic lever is open. Insert the length value based on the dimensions given. Press start button, see figure 3.5. Set lever thickness, clearances and angle according to the material thickness and type of it. If not done this, the material dimension will not accurate because of these important settings.

Figure 3.5.Prepared sample and hydraulic Shearing machine

Table 3.5.Setting for cutting samples

No	Sheet Thickness	Blade Clearance		Rake Angle	
		Min P_{os}	Max P_{os}	Material ≤ Alum .	Material ≥ Alum.
1	1.0 to 1.5 mm	1	2	0.5	1

3.6. Experimental Work on Resistance Spot Welding

The experiments were conducted at the federal technical vocational and educational training institute. Welding thickness. 0.7, 1.0, and 1.3 mm sheets of alloyed aluminum AA2017 on Hand held resistance spot welding machine with specifications, as listed in Table (3.6). The properties and composition of the workpiece sheets determined by spectrum analysis are shown in Table (3.6). Samples of dimensions 25 × 125 mm were cut from delivered sheets, with the longitudinal dimension in the rolling direction. They were welded as a lap joint ready for subsequent shear

tensile testing. A mild steel sheet with different thickness 0.6, 0.8 and 1.0mm, used to cover the aluminum alloy to be welded upper side and bottom side for transferring high current throughout the metals between the electrodes. The electrode tips (Female Cap) were of type A, according to ISO 5821-2009 and the American standard RWMA No. FF-25. They were made of zirconium–copper alloy (Cu, Cr, Zr) with the following chemical composition; Cr, 0.7–1.2%, Zr, 0.06–0.15%, bal. Cu. The electrodes were of dome configuration, Ø4 mm in diameter with a flat end.

Table 3.6.Input parameters resistance spot welding

Parameters					
Test No.	Welding current (kA)	Electrode force (kN)	Welding time (s)	Thickness of Al alloy (mm)	Thickness of cover mild steel (mm)
1	3	1.6	5	0.7	0.6
2	3	1.6	8	0.7	0.8
3	3	1.6	11	0.7	1
4	3	1.6	8	1	0.6
5	3	1.6	11	1	0.8
6	3	1.6	5	1	1
7	3	1.6	11	1.3	0.6
8	3	1.6	5	1.3	0.8
9	3	1.6	8	1.3	1

3. 7. Mechanical Tests

3.7.1. Universal Testing Machine Testing System

UTM Testing Systems are highly integrated testing packages that can be configured to meet different test needs. Each includes a load unit with an integral actuator and servo valves, a hydraulic power unit and a control system as shown in the Fig.3.6. The control system consists of three main components: the system software running on a personal computer, the digital controller and the remote-control panel. These functions work together to provide fully automated control of the test as shown figure 3.7.

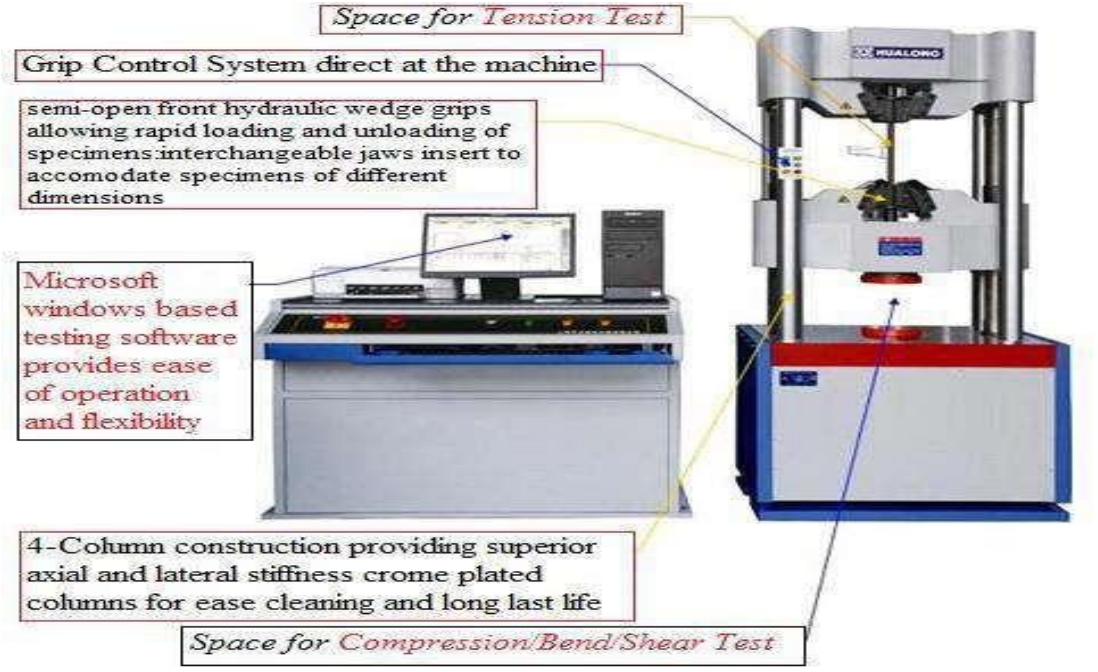

Figure 3.6. Universal Testing Machine (UTM).

A) .

B) .

Figure 3.7. Tensile test A) Sample and B) Testing process

3.7.2. Hardness Test

The main aim of this test is specifying the hardness number for base metal, welded zone and the heat affected zone (HAZ). The specimen preparation included grinding and polishing according to [ASTM E90-82, 2003]. A load of (200 g) was employed and a dwell time was (15sec). Micro hardness locations have been taken along straight-line start.

➢ **Rockwell Hardness Testing Machine**

The Rockwell hardness test method consists of indenting the test material with a diamond cone or hardened steel ball indenter. The indenter is forced into the test material under a minor preliminary load and the permanent effect is studied to know the hardness of the sample material.

Rockwell Testers come in a wide range of models depending on their operations and a variety of test forces they can apply during tests. These testers provide accurate results even after rough handling of test tables or test pieces.

Figure 3.8. Digital hardness tester machine and testing process

It measures the Leeb value (L) for materials, which is a ratio of the impact velocity to the rebound velocity, see figure 3.9. Hardness measurements are carried out by a dynamic method, which allows testing on areas of difficult access in this study use this process to compare the hardness between the welding area and the normal work piece.

Figure 3.9. Brinell hardiness tester.

3.7.3. The Optical Microscope

The optical microscope, also referred to as a light microscope, is a type of microscope. A digital microscope is a microscope equipped with a digital camera allowing are 10× and 100× respectively, giving a final magnification of 1,000×. Long focus microscope with camera adapter see figure 3.10.

Figure 3.10. Micro structure testing process and optical microscope

3.8. Taguchi Method

Taguchi is an engineer and statistician, where the Taguchi methods are statistical methods developed by Taguchi to improve the quality of manufactured goods and, more recently, to a different field of an area like biotechnology, marketing, and advertising (Jana N. et al. 2009 and Vikas P. et al. 2013).

3.8.1. Description of the Taguchi Method

The proposed that engineering optimization of a process or product should be carried out in a three-step approach: 1. System Design, 2. Parameter design, and 3. Tolerance design. In system design, the engineer applies scientific and engineering knowledge to produce a basic functional prototype design, this design includes the product design stage and the process design stage.

Since system design is an initial functional design, it may be far from optimum in terms of quality and cost. Following from system design is parameter design. The objective of parameter design is to optimize the settings of the process parameter values for improving quality characteristics and to identify the product parameter values under the optimal process parameter values. Besides, it is expected that the optimal process parameter values obtained from parameter design are insensitive to variation in the environmental conditions and other noise factors (Jana N. et al. 2009).

Finally, tolerance design is used to determine and analyze tolerances around the optimal settings recommended by the parameter design. Tolerance design is required if the reduced variation

obtained by the parameter design does not meet the required performance, and involves tightening tolerances on the product parameters or process parameters for which variations result in a large negative influence on the required product performance. However, based on the above discussion, parameter design is the key step in the Taguchi method to achieving high quality without increasing cost.

3.8.2. Taguchi Methods for Design of Experiments

In this study, experiments are designed using the Taguchi method with L9 orthogonal array. Three process parameters with three levels, including the thickness of the workpiece, thickness of the the cover sheet, and welding time are applied (Jana N. et al. 2009 and Vikas P. et al. 2013).

By using the Taguchi method (L9, Orthogonal Array) as a DOE tool, and made the parameters above as variables in the experimental works, the weld process modeling is applied for each thickness (0.7mm, 1mm and 1.3 mm) aluminum alloy and the cover material is mild steel thickness of (0.6mm, 0.8mm and 1mm). The process variables and notations are shown in table (3.6). The maximum temperature, tensile strength and hardness of the welded area are the process responses. The characteristics ‘‘larger is better’’ for signal-to-noise ratio is considered for process response.

3.9. FEM Model for Resistance Spot Welding Process

- Steps followed FE Simulation

The early simulation works were generally on RSW Aluminum alloy plate. As the use of aluminum alloy sheets has increased rapidly in recent years in the automotive body assembly, research on RSW aluminum, including numerical simulation, has attracted more attention. The basic physical principles remain the same for resistance spot welding copper and aluminum alloys, so do the fundamental equations for simulation. However, there are major differences in the physical processes between welding aluminum alloys and copper, mainly due to their differences in mechanical, thermal, electrical, and metallurgical properties.

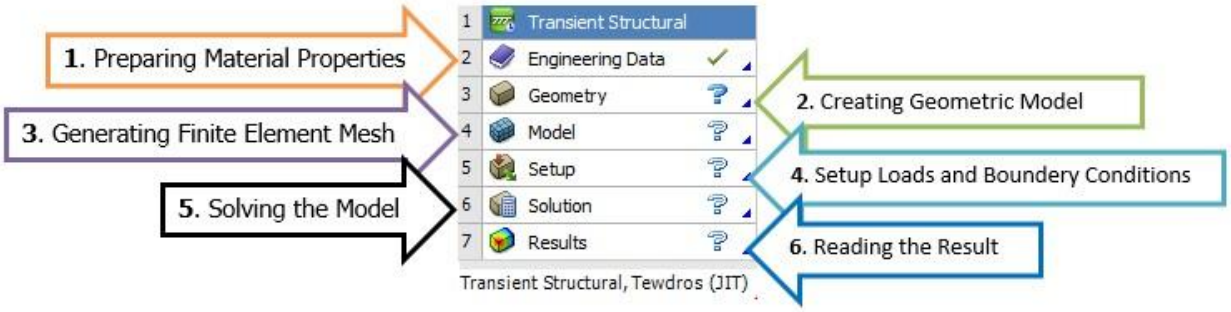

Figure 3.11. General approach of ANSYS workbench working window shown below.

Step 1. Selecting the physics used at resistance spot welding, form Analysis system box.

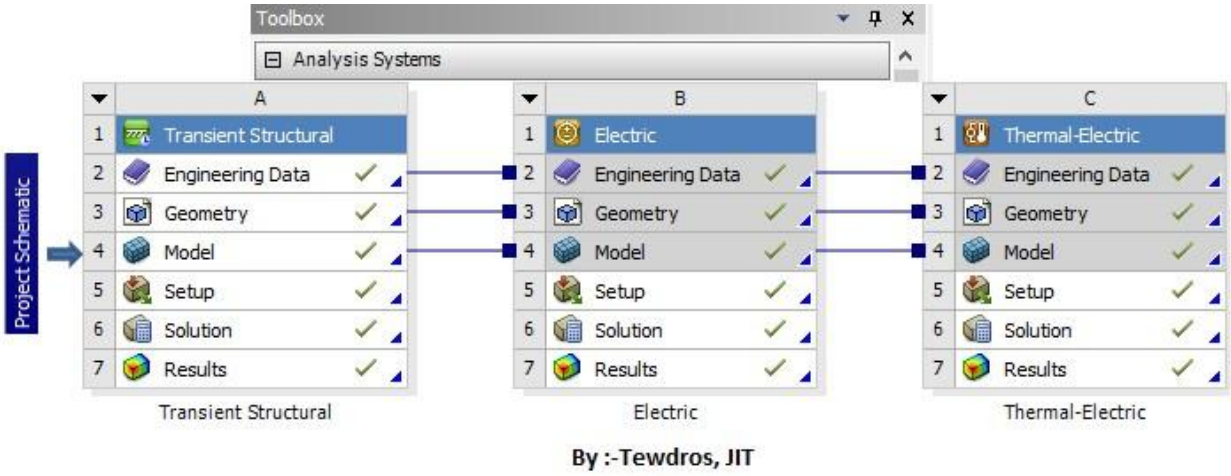

Figure 3.12. Analysis system on workbench

Step 2. Creating the Model

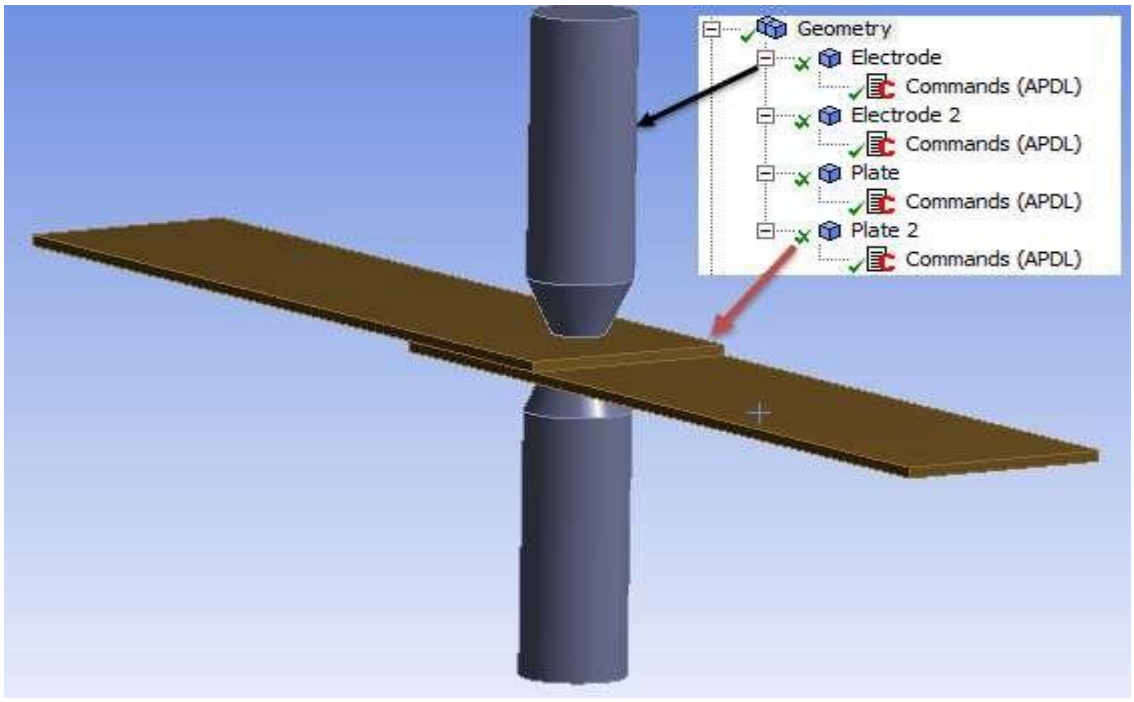

Figure 3.13. Model Generation renaming each part of RSW.

Step 3. Assigning material/ importing new material if not available on the material library of the software.

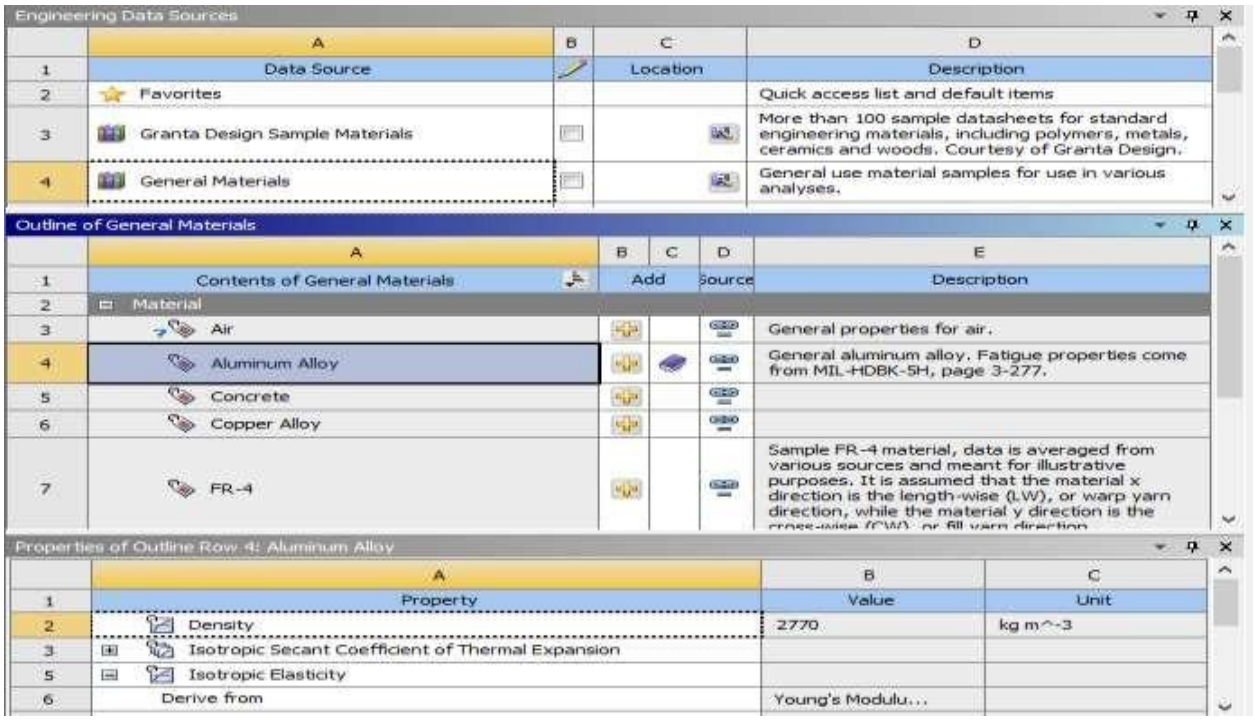

Figure 3.14. Setting the material and importing new material

Step 4. Setting proper contact between parts (Copper Electrode and Aluminum alloy plates).

There are five types of contact setting, Bonded, No separation, Rough, Frictionless, Frictional. A surface-to-surface contact discretization is used to formulate the contact between parts, and a master-slave surface pair has been established for each contact pair. This technique of contact formulation avoids big and undetected penetrations into the slave surface from nodes on the master surface, resulting in more precise stress outcomes compared to other methods. So for RSW the most common contact setting is No separation and Newton Raphson mathematical formulation is used by most researchers.

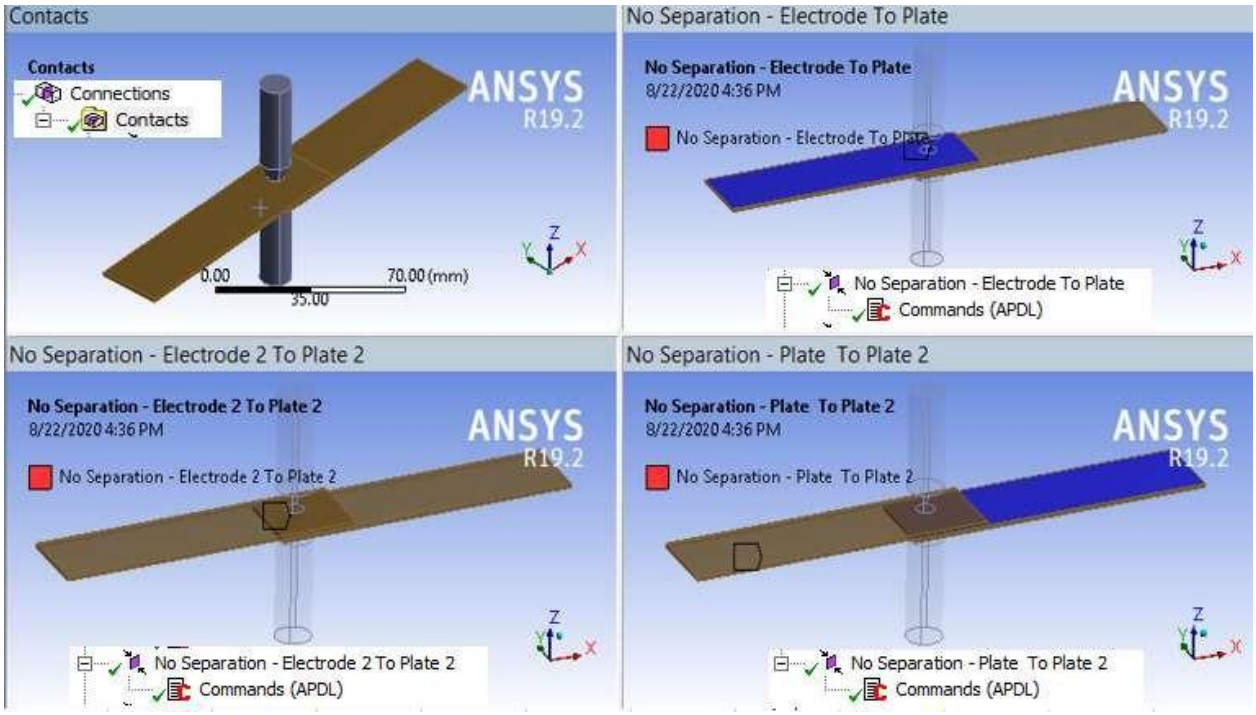

Figure 3.15. Contact setting

Step 5. Meshing (Discretization), selecting best meshing techniques for doing welding so that tetrahedral meshing is used for this simulation see figure 3.16. Discretizing complex geometries like curvatures on surfaces in FEM curved boundaries can be closely simulated using various types of elements, such as triangular (for plane problems) or tetrahedral (for three-dimensional problems) elements. 1-D spot weld elements cannot satisfactorily describe propagation and energy absorption of weld. To analyses model precisely detail solid mesh model developed. This model consider spot weld geometry and heterogeneity of material and so it is physically more accurate model.

This Model has shell elements in the plate whereas spot weld used 8-node solid elements. Coupling of the two element types is done [Mc Cun et al. and Shim K. et al.]. The rotations and displacements of the shell nodes are compatible with the displacements of the solid element nodes by constraining DOF of the shell and solid nodes. Simplified spot weld model represented by single hex spot weld. Hex spot weld model provides significant savings in terms of reduced modeling.

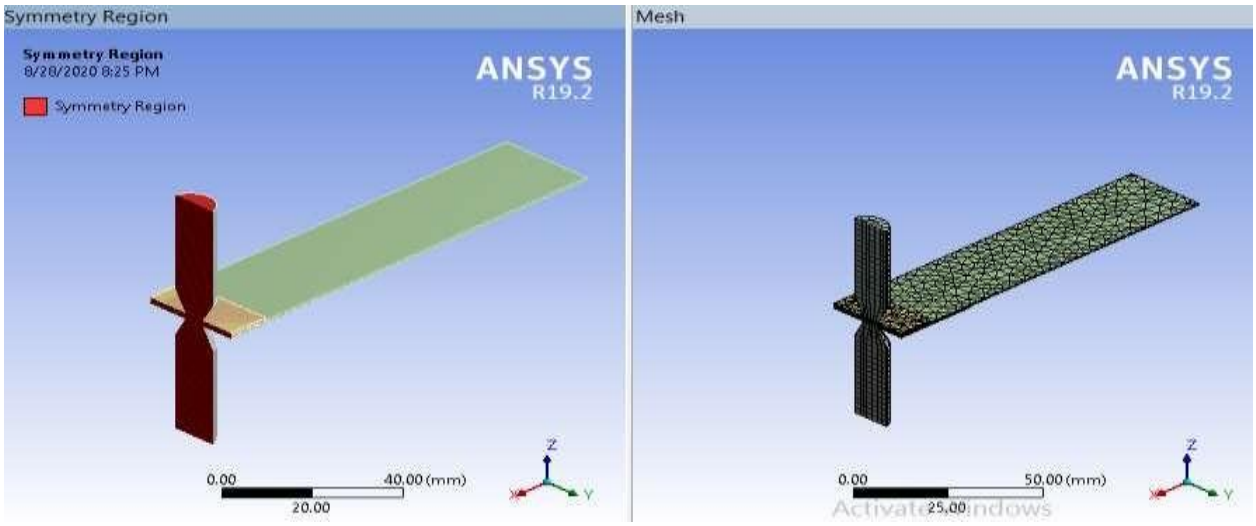

Figure 3.16. Generated mesh and symmetry of the FE model.

Step 6. Checking for Quality of Meshing

To reduce runtime when adjusting the models, loads and boundary Figure 3.17 showing the quality of the elements in all the model regions. All around joint have higher or equal to 0.70 element quality. The choice for element quality compromises a combined quality metric between 0 and 1. A value of 1 designates a perfect cube or square while a value of 0 shows that the element has a zero or negative volume.

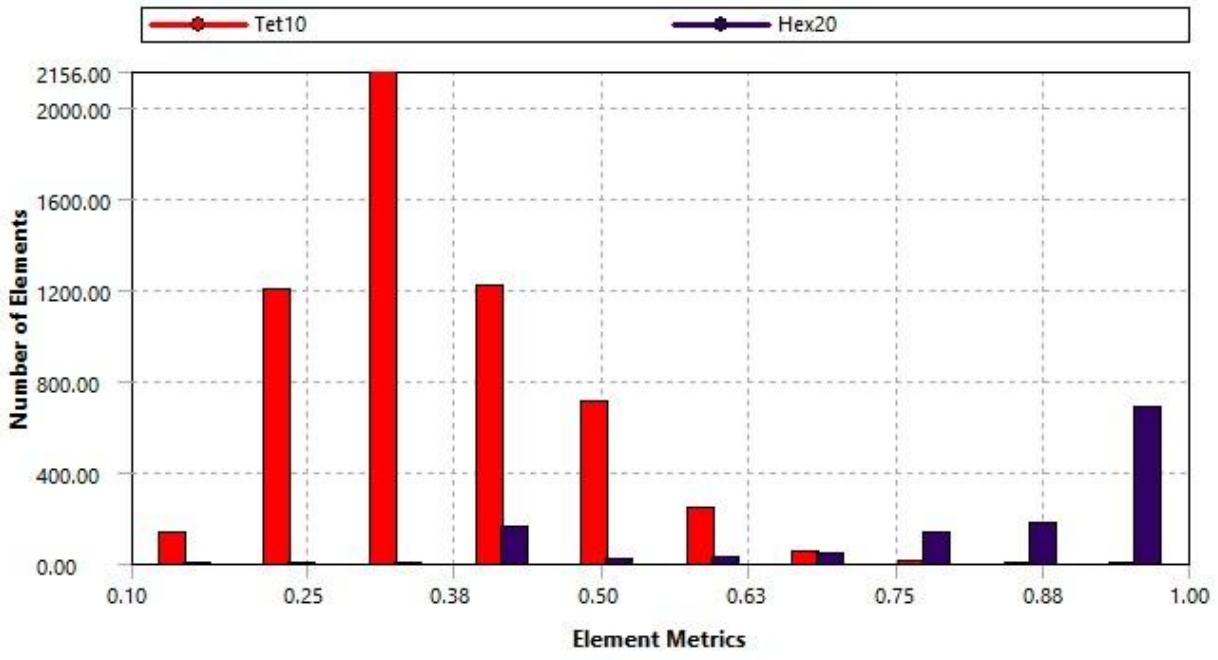

Figure 3.17. Checking quality of mesh

Step 7. Boundary conditions: - Thermal boundary conditions the free convection and radiation from the exterior face of the electrode and power input to the tip. Values of the convective heat transfer coefficients in free air varied from 5 to 25 W/m^2-K, with a zero value simulating a completely insulated condition. The effect of the magnitude of the heat transfer coefficient on the maximum tip surface temperature. These values were calculated using steady-state thermal analysis, ignoring radiation. It appears that convection in free air is not important; therefore, unless otherwise noted, convection in free air will not be considered further. The convective heat loss from the exterior surface can be found by Newton's Law of cooling.

$$\boldsymbol{Q_i = hA_i(T_i - T_o)} \text{.....Eq.1}$$

Where h is the convective heat transfer coefficient. (For free convection in air, h has a maximum value of 25 W/m^2-K as mentioned above.) Q_i Denotes the heat loss on surface **i** with areaA_i, T_i is the temperature on surface A_i and T_o is the ambient temperature. With an ambient temperature of 200°C (392°F) and T_i obtained from the temperature distribution in the electrode, a maximum total convective heat loss from the weld cap can be estimated. The total heat loss was found to be 7.25 **W**, which would cause a tip surface temperature change of less than ~2°C (~35.6°F). The net

radiant heat exchange of an ideal black body from surface **i** and its surroundings, with an absolute temperature of T_o, is given by the Stefan-Boltzmann equation:

$$\boldsymbol{E_i = \sigma \in A_i\left(T_i^4 - T_o^4\right)} \text{.....Eq.2}$$

$$E_i = 5.67 * \left(\left({}^{T_i}/_{100}\right)^4 - \left({}^{T_o}/_{100}\right)^4\right)$$

In this equation, T_i is the absolute temperature of body surface **i,** is a constant with a value of 5.67* 10^{-8} W/m^2-K, and K is the emissivity. For an ideal black body, ∈ has a value of 1.0. Estimates of the maximum radiant heat loss from the weld cap. The radiant heat loss is even less than the convective heat loss. (Since the maximum convective heat loss contributed to a temperature change of <2°C (<35.6°F), the radiant heat loss was not considered in this analysis.

This study made use of experimentally determined values for power dissipation at the electrode/workpiece interface in spot welding of aluminum alloy AA 17. A typical power dissipation curve (obtained during SW an aluminum alloy AA -2017 with a current of 3 kA).

Step 8. Analysis Setting inserting time step size/ loading step size, checking time step on, large deformation on, and make solver Iterative than direct solver because no accurate solution by direct solver for complex geometry and operation see figure 3.18.

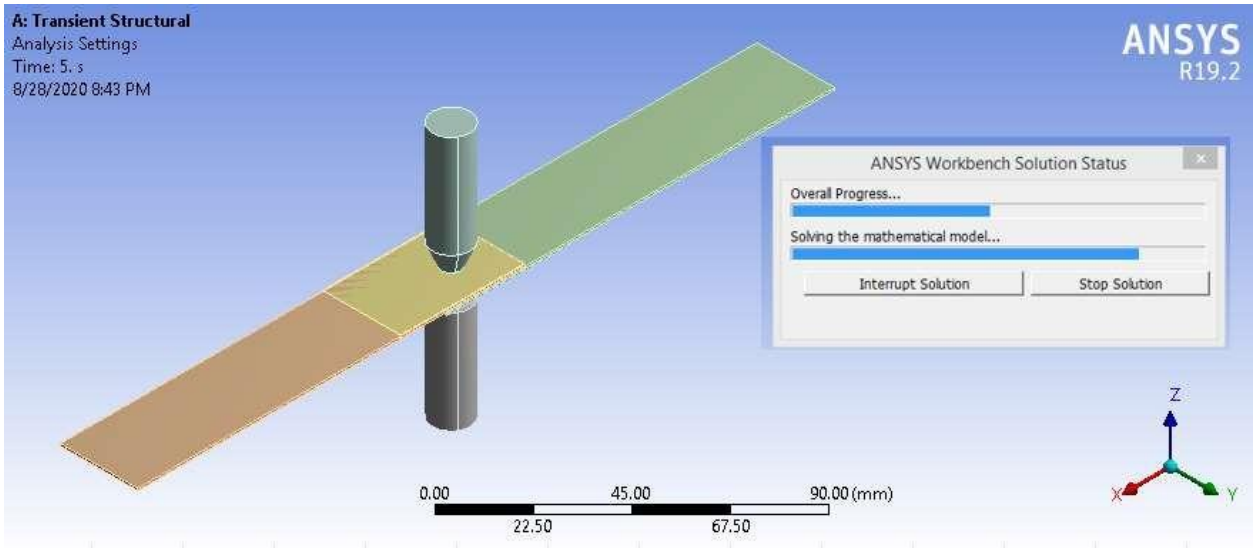

Figure 3.18. Setting the analysis and solving the mathematical model

CHAPTER FOUR

4. Results and Discussions

4.1. Introduction

Under this chapter the main finding of both Experimental and finite element analysis results and clearly discussed.

4.2. Experiments Results

The experimental results are based on the following input parameters: - thickness of aluminum sheet (0.7, 1, and 1.3) mm, cover sheet (0.6, 0.8, and 1) mm, welding current (3kA), Electrode Force (1.6kN), and electrode tip diameter (4) mm, welding time (5, 8 and 11) seconds. Hence, nine (9) tests are done by putting in to three different test groups based on Aluminum weld sheet and weld cover sheet thickness.

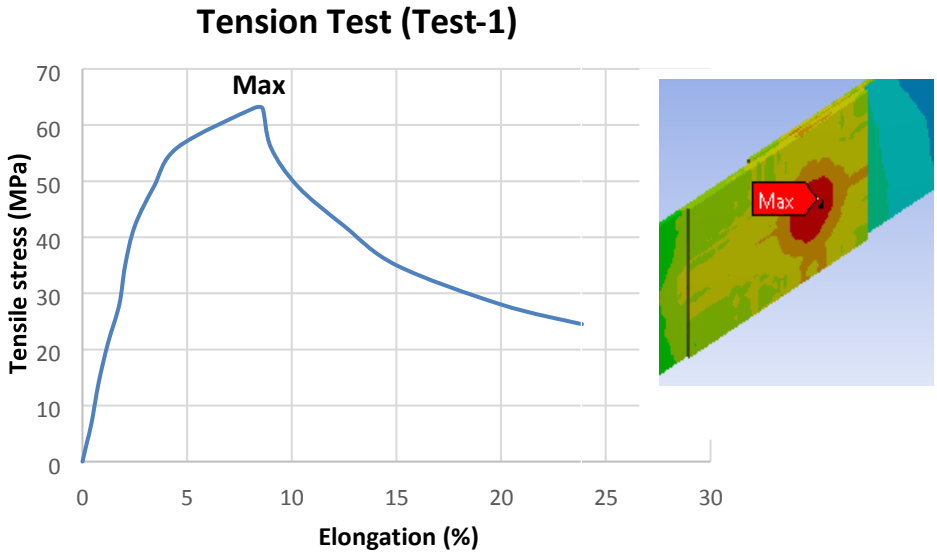

Figure 4.1. Tensile test result specimen number 1

As show in Figure 4.1., tension Test-1 the plot of stress versus strain have linear relation up to elastic limit, the maximum stress is above 60MPa on the given experiment similarly the maximum stress obtained on FEA is 68MPa which is good correlation of the result obtained.

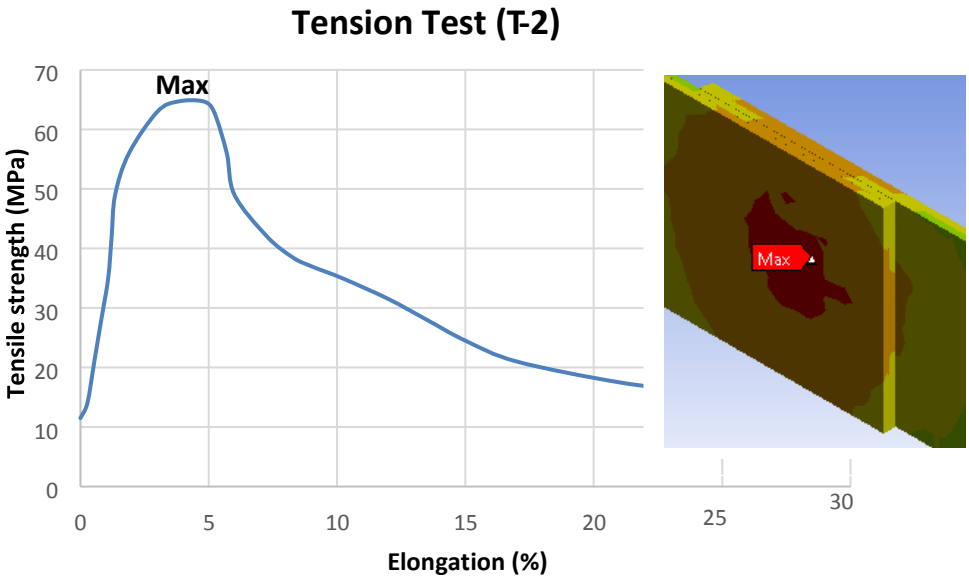

Figure 4.2. Tensile test result specimen number 2

For experimental tension test on specimen 2, as shown in figure 4.2., stress versus stain have linear relation up to elastic limit then the maximum stress is above 60Mpa as shown on stress –strain curve and which is similar maximum stress result obtained on FEA, 73MPa, shows that good correlation with experimental test result.

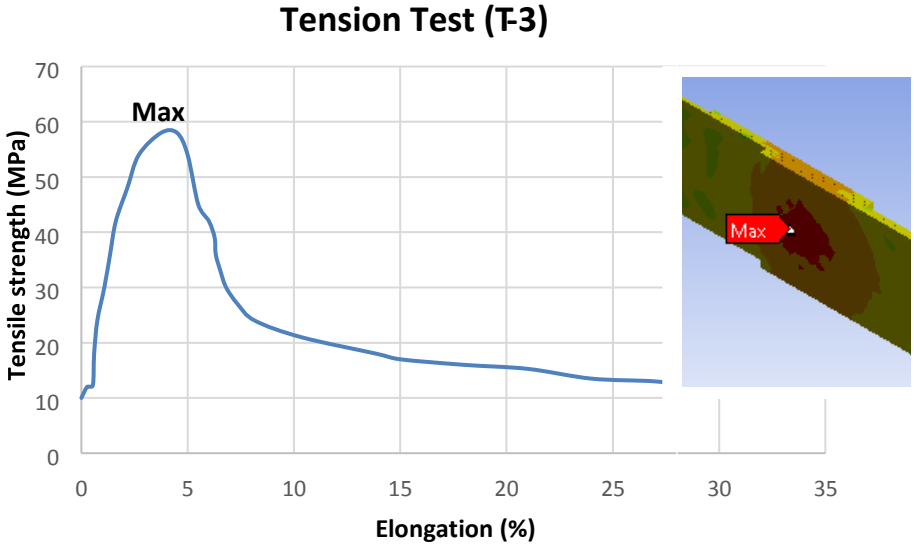

Figure 4.3. Tensile test result specimen number 3

For experimental test on specimen 3 the stress stain curve shows linear relation up to elastic limit and gets its maximum above 55MPa and may be due to welding time and some experimental constraints there is small variation on the maximum value of stress on FEA.

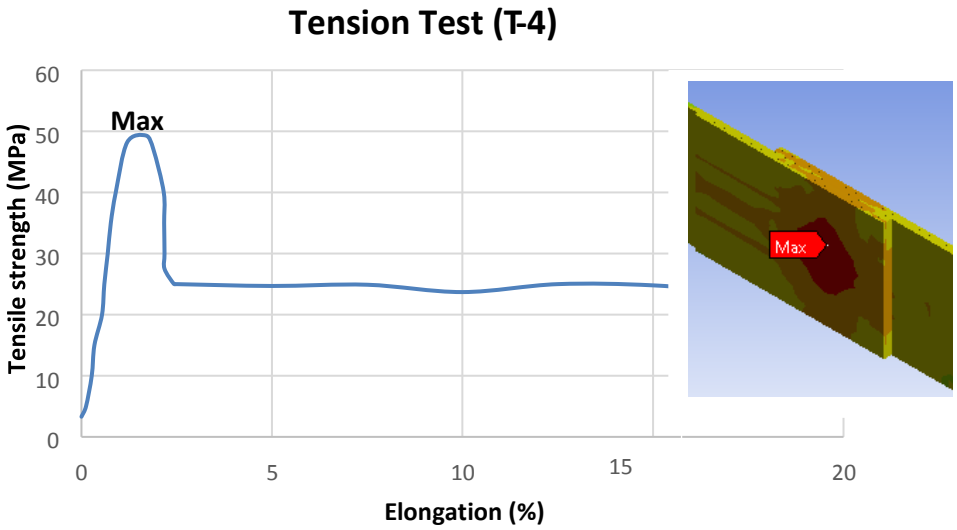

Figure 4.4. Tensile test result specimen number 4

Experimental test on specimen 4 as shown figure 4.4., stress and strain have linear relation they have up to elastic limit and then the maximum stress is above 40MPa, may be due to experimental constraints like welding time, thickness of weld sheet, cover sheet makes smaller variation with FEA result obtained.

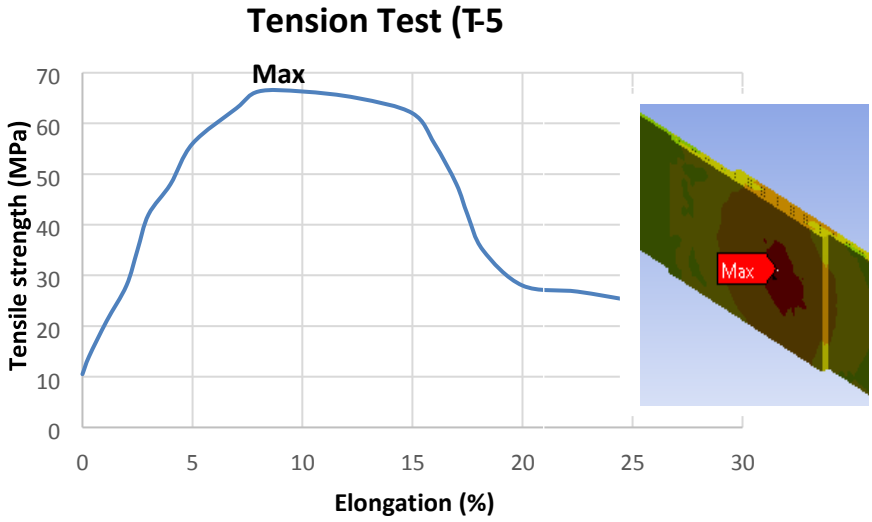

Figure 4.5. Tensile test result specimen number 5

Experimental test on specimen 5 as shown figure 4.5., stress and strain have linear relation they have up to elastic limit and then the maximum stress is above 60MPa, which is similar with FEA result obtain 76MPa, this shows good for validation of FEA result obtained.

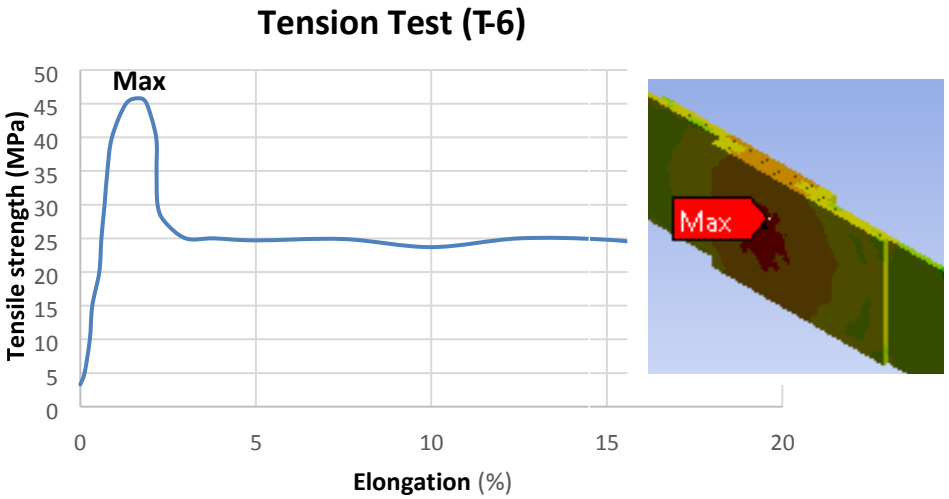

Figure 4.6. Tensile test result specimen number 6

Experimental test on specimen 6 as shown figure 4.6., stress and strain have linear relation they have up to elastic limit and then the maximum stress is above 40MPa, may be due to experimental constraints like welding time, thickness of weld sheet, cover sheet makes smaller variation with FEA result obtained.

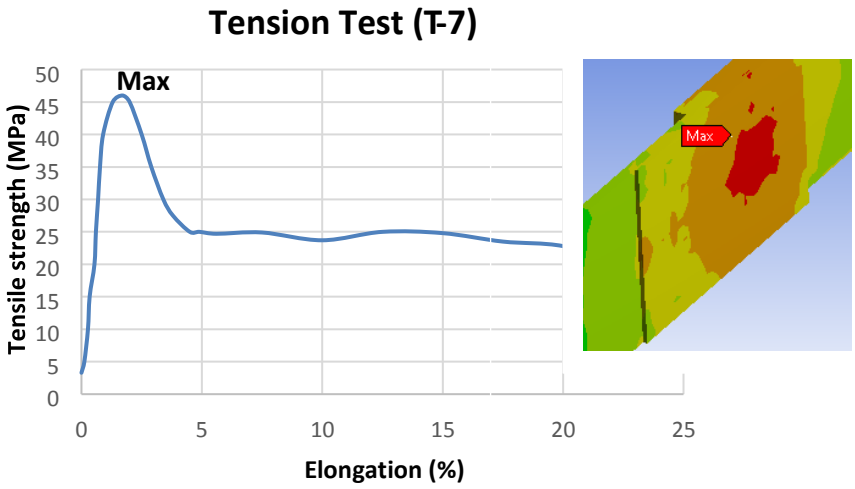

Figure 4.7. Tensile test result specimen number 7

Experimental test on specimen 7 as shown figure 4.7., stress and strain have linear relation they have up to elastic limit and then the maximum stress is above 40MPa, may be due to experimental constraints like welding time, thickness of weld sheet, cover sheet makes smaller variation with FEA result obtained.

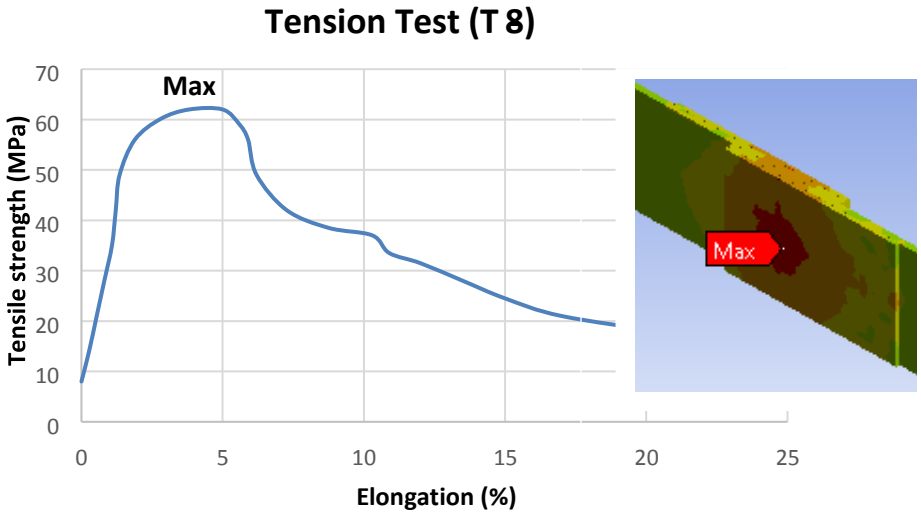

Figure 4.8. Tensile test result specimen number 8

Experimental test on specimen 8 as shown figure 4.8., stress and strain have linear relation they have up to elastic limit and then the maximum stress is above 60MPa, which is similar with FEA result obtain 78MPa, this shows good for validation of FEA result obtained.

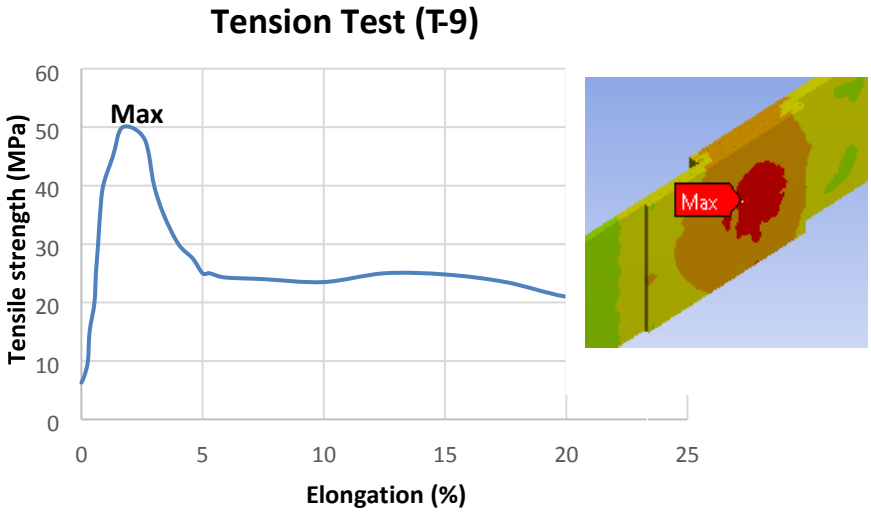

Figure 4.9. Tensile test result specimen number 9

Experimental test on specimen 9 as shown figure 4.9., stress and strain have linear relation they have up to elastic limit and then the maximum stress is above 50MPa, may be due to experimental constraints like welding time, thickness of weld sheet, cover sheet makes smaller variation with FEA result obtained.

4.3. Result of FEA

The result of finite element analysis on the following experimentally validated specimen sizes taken as study parameters are done, Aluminum alloy weld sheet thickness (0.7, 1 and 1.3) mm, Mild steel weld cover thickness (0.6, 0.8 and 1) mm and constant diameter of Copper alloy electrode on boundary conditions such as electrode force 1600N, welding current 3KA, welding time (5, 8 and 11) seconds. Therefore, the response is recorded as discussed on figure 4.10-4.19.

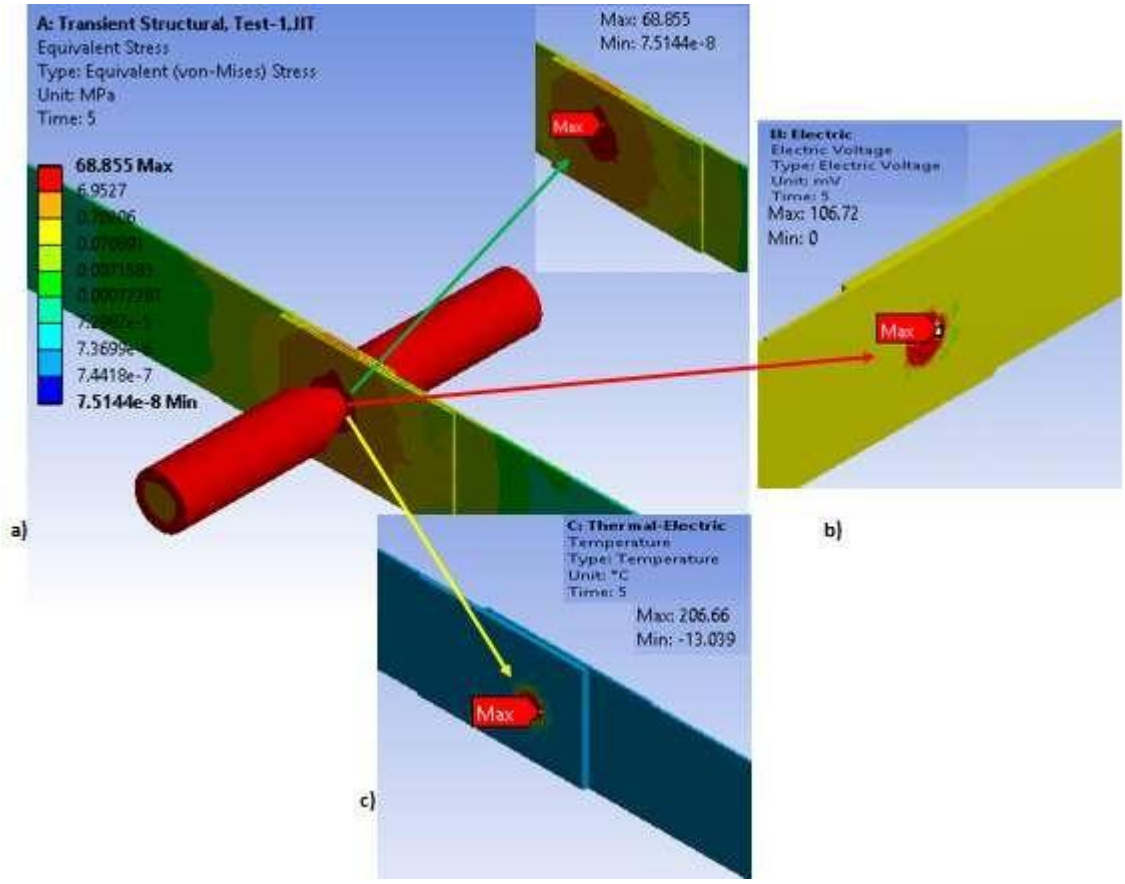

Figure 4.10. Test-1, a). Von-Misses stress (MPa), b). Voltage (mV), and c). Temperature in ℃, of Simulation of RSW

Figure 4.10a, shows that von misses stress around the weld region is getting maximum (68.85MPa) as compared to other location on the weld sheet, which is due to weld zone. `

Figure 4.10b, shows that electric voltage around the weld region, which is maximum (106.72mV).

Figure 4.10c, shows temperature distribution around the weld region which maximum (206℃) as compared to other location s on the weld sheet.

As compared to the response of specimen 2 and 3, for same welding current, electrode force and thickness of aluminum alloy weld sheet, variation of welding time strongly affecting the welding temperature, maximum principal stress and electrode in weld area. Therefore, due to less welding time and less cover sheet thickness, the weld joint response is less as shown in figure 4.10, as compared to figure 4.11 and 4.12.

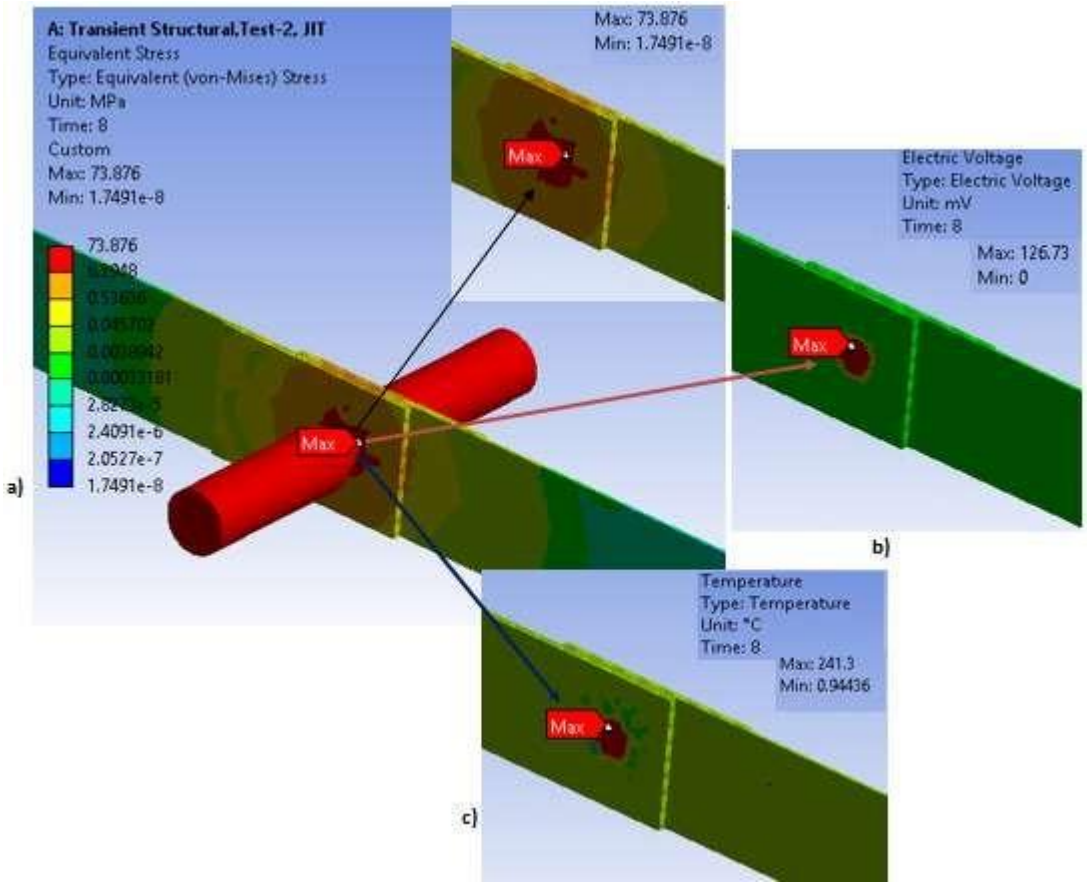

Figure 4.11. Test-2, a). Von-Misses stress (MPa), b). Voltage (mV), and c). Temperature in ℃, of Simulation of RSW

Figure 4.11a, shows that von misses stress around the weld area is getting maximum (73.86MPa) as compared to other location on the weld sheet. `

Figure 4.11b, shows that electric voltage around the weld, which is maximum (126.73mV).

Figure 4.11c, shows temperature distribution around the weld region which maximum (241.3℃) as compared to other locations on the weld sheet.

As shown on figure 4.11, the test is done for constant welding current, electrode force and aluminum sheet thickness, increasing of weld time and thickness of cover sheet in RSW causing an increment on the welding joint responses.

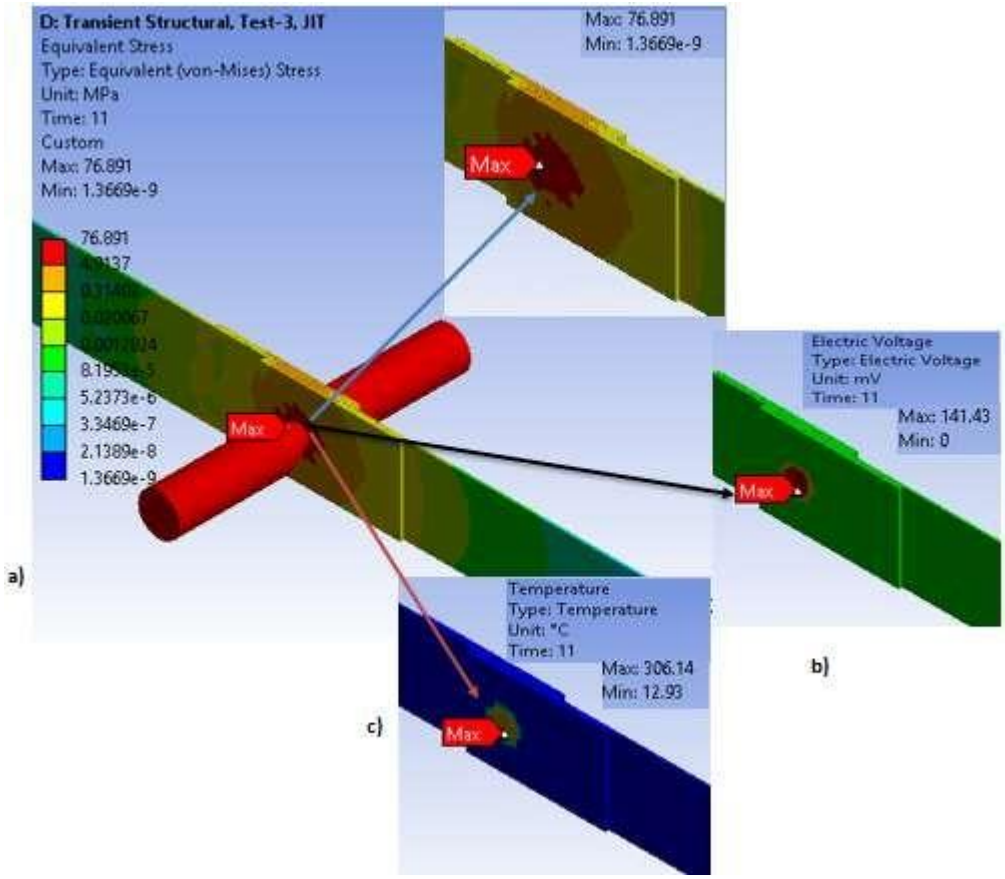

Figure 4.12. Test-3, a). Von-Misses stress (MPa), b). Voltage (mV), and c). Temperature in ℃, of Simulation of RSW

Figure 4.12a, shows that von misses stress around the weld is getting maximum (76.89MPa) as compared to other location on the weld sheet. `

Figure 4.12b, shows that electric voltage around the weld, which is maximum (141.43mV).

Figure 4.12c, shows temperature distribution around the weld region which maximum (306.14℃) as compared to other location s on the weld sheet.

For constant welding current, electrode force and aluminum sheet thickness, increment on welding time and weld cover sheet thickness causes increment on the response of weld zone as shown in figure3. In above three specimens as shown in figure 4.10, 4.11 and 4.12, for constant welding current, electrode force and aluminum sheet thickness, weld joint responses in von-Misses stress is (68.86,73.88 and 76.89) MPa respectively, Electric Voltages (106.72,126.73 and 141.43) mV, respectively and Weld temperature (206.66,241.30 and 306.14) ℃, respectively. Specimen 3 have maximum values of the joint response, may be due to an increment on cover sheet thickness and weld time. Since these two parameters are the determining factors in RSW.

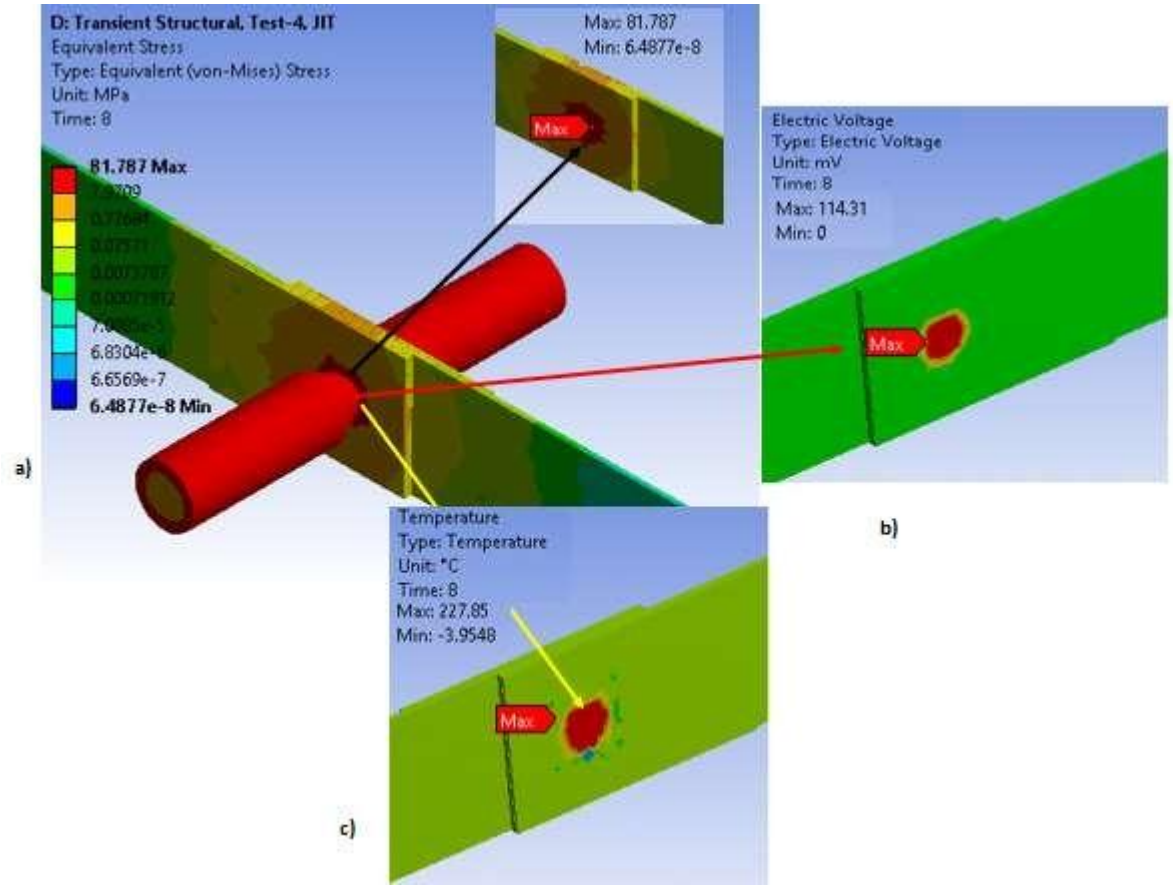

Figure 4.13. Test-4 a). Von-Misses stress (MPa), b). Voltage (mV), and c). Temperature in ℃, of Simulation of RSW

Figure 4.13a, shows that von misses stress around the weld is getting maximum (81.787 MPa) as compared to other location on the weld sheet.

Figure 4.13b, shows that electric voltage around the weld, which is maximum (114.31 mV).

Figure 4.13c, shows temperature distribution around the weld which maximum (227.85℃) as compared to other location s on the weld sheet.

Figure 4.13, shows maximum values of weld joint responses as compared to specimen 1, 2 and 3, that may be due to increment on aluminum sheet thickness from 0.7mm to 1mm. But in case of specimen 4, when aluminum sheet thickness, electrode force and welding current held constant variation of cover sheet thickness and welding time have an effect on weld joint response as shown in specimen 4,5, and 6.

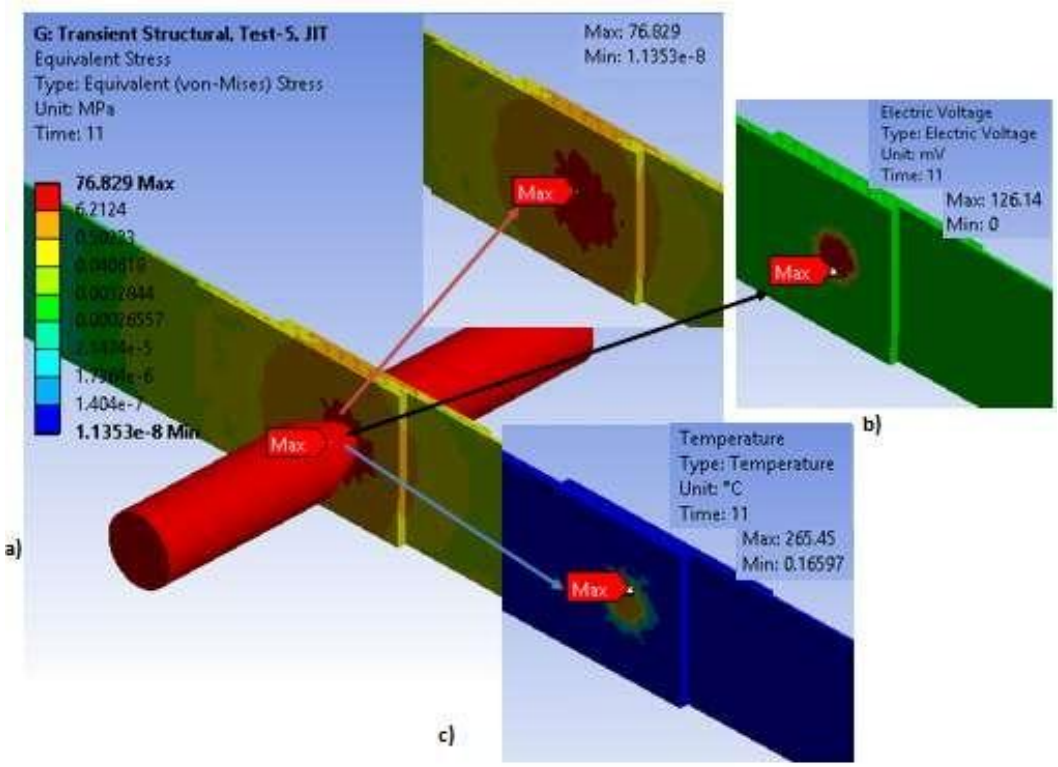

Figure 4.14. Test-5, a). Von-Misses stress (MPa), b). Voltage (mV), and c). Temperature in ℃, of Simulation of RSW

Figure 4.14a, shows that von misses stress around the weld is getting maximum (76.83MPa) as compared to other location on the weld sheet. `

Figure 4.14b, shows that electric voltage around the weld, which is maximum (126.14mV).

Figure 4.14c, shows temperature distribution around the weld which maximum (265.45℃).

For constant weld plate thickness, electrode force and weld current, decrement on weld cover sheet thickness affect the von-Misses stress and electric voltage of the weld zone, but weld temperature is increased as compared to specimen 4, which is may be due to increment on weld time.

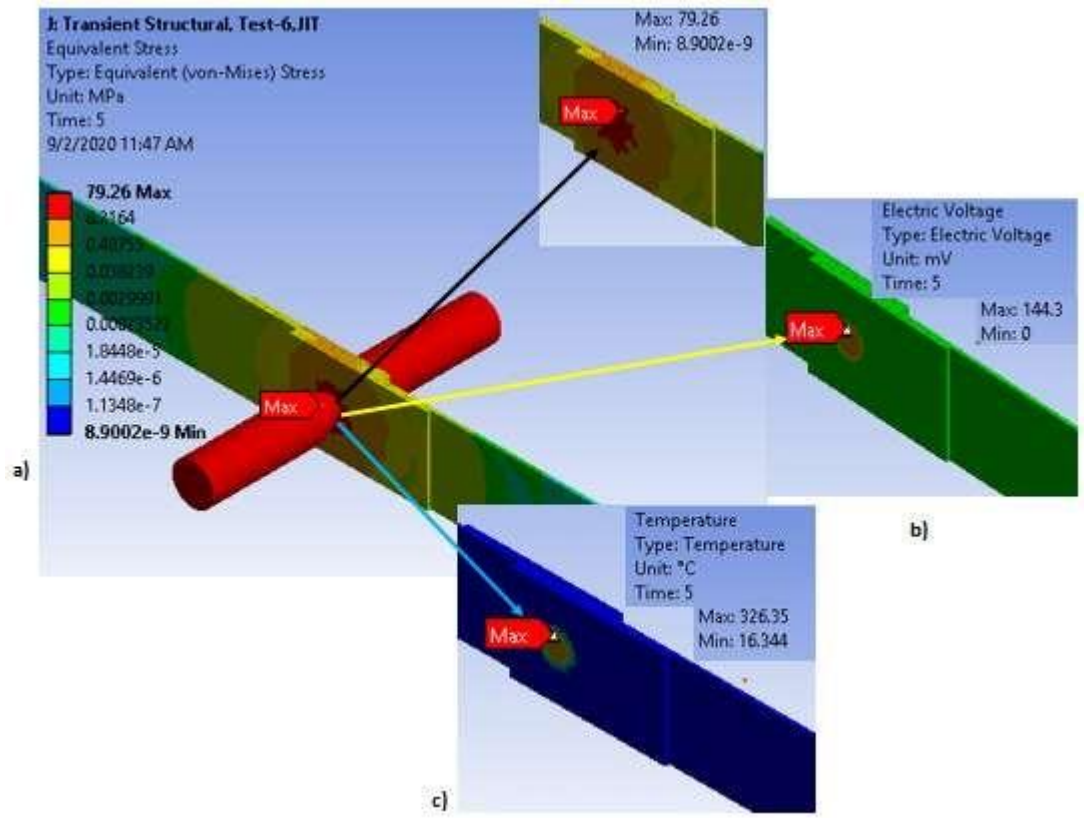

Figure 4.15. Test-6, a). Von-Misses stress (MPa), b). Voltage (mV), and c). Temperature in ℃, of Simulation of RSW

Figure 4.15a, shows that von misses stress around the weld is getting maximum (79.26MPa) as compared to other location on the weld sheet.

Figure 4.15b, shows that electric voltage around the weld, which is maximum (144.3mV).

Figure 4.15c, shows temperature distribution around the weld which maximum (326.35℃).

As shown in figure 4.15, as specimen 4 and 5, for constant aluminum sheet thickness, electrode force and weld current, an increment on cover sheet thickness have influence on the weld joint response. Hence, from specimen 4, 5 and 6, for same aluminum sheet thickness, electrode force and weld current, increment or decrement on cover sheet thickness and weld time have significant effect on RSW joint response on von-Misses stress (81.79, 76.83 and 79.26) MPa, respectively,

Electric voltage (114.31, 126.11 and 144.30) mV, respectively, and weld temperature distribution around the weld zone (227.85, 265.45 and 326.35) ℃, respectively.

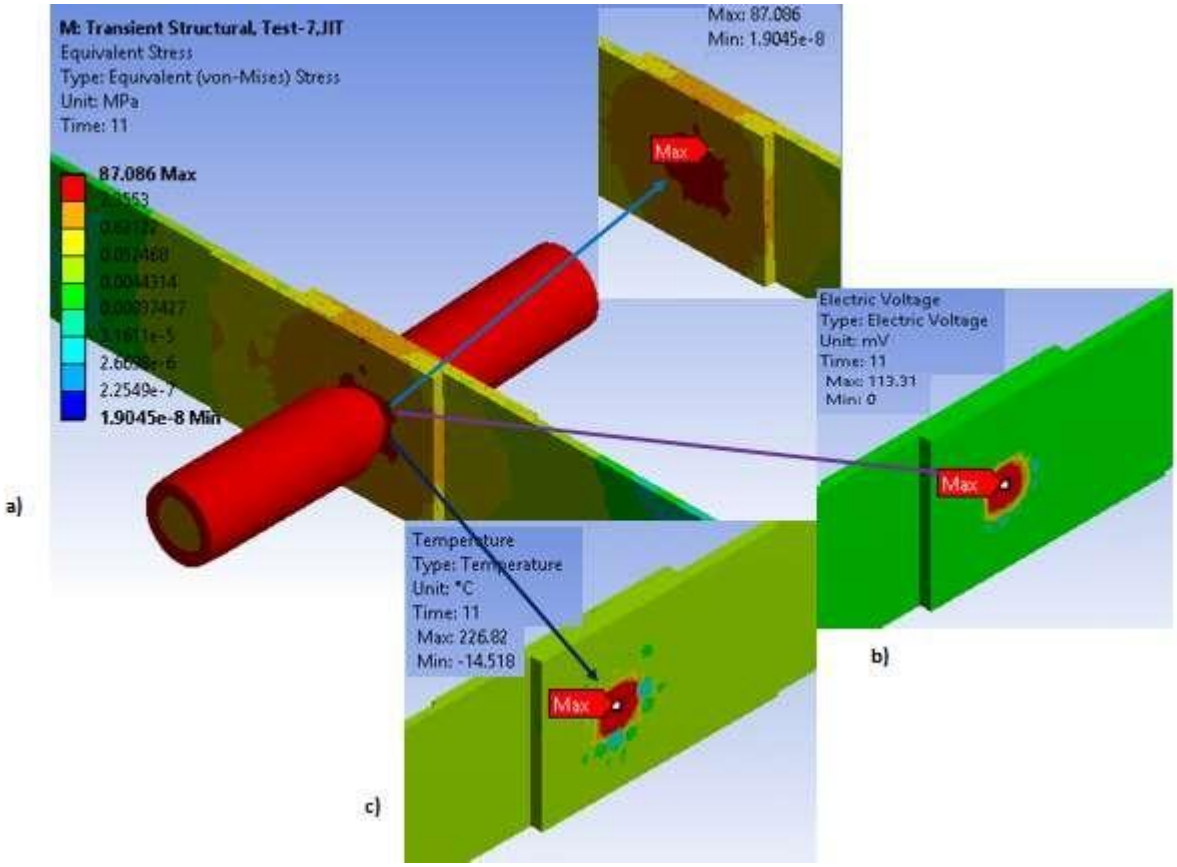

Figure 4.16. Test-7, a). Von-Misses stress (MPa), b). Voltage (mV), and c). Temperature in ℃, of Simulation of RSW

Figure 4.16a, shows that von misses stress around the weld is getting maximum (87.09MPa) as compared to other location on the weld sheet.

Figure 4.16b, shows that electric voltage around the weld, which is maximum (113.31mV).

Figure 4.16c, shows temperature distribution around the weld which maximum (226.82℃) as compared to other location s on the weld sheet.

For specimen 7, as shown in figure 4.16, the increment on thickness of aluminum sheet is causing, variation on the RSW responses as compared to the above tests on weld sheet thickness on 0.7 and 1mm. But for constant weld specimen size 1.3mm, electrode force (1.6KN) and weld current

(3KA) the response of temperature variation is proportional but von-Misses stress around the weld is not, that is may be due to welding time which is maximum weld time (11second).

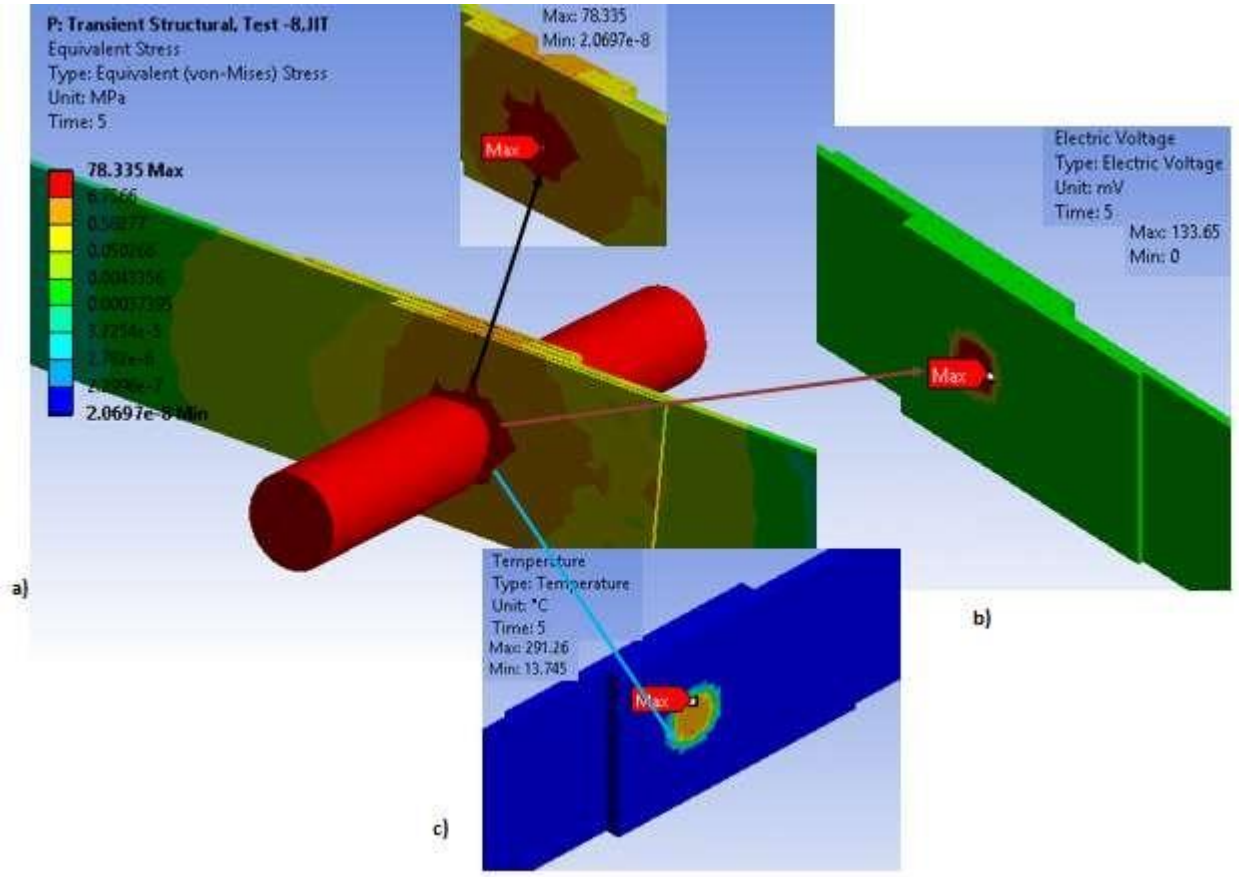

Figure 4.17. Test-8, a). Von-Misses stress (MPa), b). Voltage (mV), and c). Temperature in ℃, of Simulation of RSW

Figure 4.17a, shows that von -Misses stress around the weld is getting maximum (78.33MPa) as compared to other location on the weld sheet. `

Figure 4.17b, shows that electric voltage around the weld region, which is maximum (133.65mV).

Figure 4.17c, shows temperature distribution around the weld region which maximum (291.26℃).

As shown in figure 4.17, specimen 8, the test is done for constant current, electrode force and aluminum weld sheet thickness, the response on RSW is varied in such way that welding temperature and electric voltage distribution around the weld zone have direct relation with weld joint response. So that, it shows an increment in both weld cover sheet causes the weld zone

temperature and electric voltage increment irrespective of the weld time and von-Misses stress is strongly affected by welding time as shown summery Table 4.2.

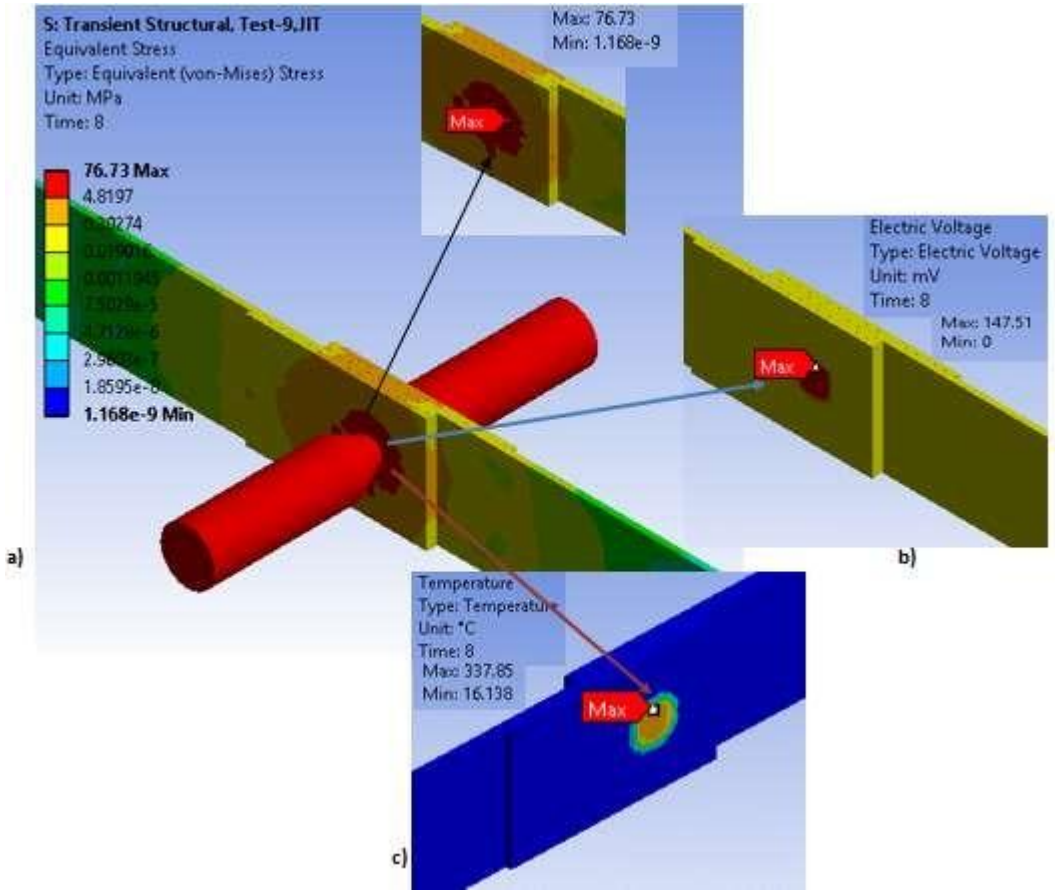

Figure 4.18. Test-9, a). Von-Misses stress (MPa), b). Voltage (mV), and c). Temperature in ℃, of Simulation of RSW

Figure 4.18a, shows that von misses stress around the weld is getting maximum (76.73MPa) as compared to other location on the weld sheet.

Figure 4.18b, shows that electric voltage around the weld, which is maximum (147.51mV).

Figure 4.18c, shows temperature distribution around the weld which maximum (337.85℃) as compared to other location s on the weld sheet.

On last test specimen 9, as shown in figure 4.18, for constant welding current, weld sheet thickness and electrode force, electric voltage and temperature distribution at weld zone is increases irrespective with welding time.

To summarize the FEA simulation response of the RSW, nine (9) specimens are tested both experimentally and numerical laboratory to validate the research finding. Hence, as shown on above results of simulation, when FEA on RSW of mild steel covered Aluminum sheet welding, nine (9) specimens were simulated by using the physics called Transient Structural-Electric and Thermal, to get the following response which were listed in Table 4.1. Figure 4.10-4.18 shows the Von Mises stress distribution in RSW progress. Shows that, the maximum stress has occurred at edge of the electrode. Non-uniform stress distribution also occurred at contact area between electrode and weld metal which phenomena was reported a lot in other study [Nied A. and Tsai, et al.]. The reason for this phenomenon is due to the electrode was not assumed rigid body but deformable body. If the electrode has assumed rigid body, the stress singularity which cause to divergence problem has occurred at the edge of the electrode.

Table 4.1.Summery on simulation results of RSW.

Specimen No.	Max. Welding Temp. (℃)	Max. Von misses stress (MPa)
#1	206.66	68.86
#2	241.30	73.88
#3	306.14	76.89
#4	185.01	81.79
#5	265.45	76.83
#6	326.35	79.26
#7	220.14	87.08
#8	255.26	78.33
#9	337.85	76.73

4.4. Precision of Prediction

The reasonable benchmark to check the accuracy of each FEM is to compare the model predicted values with experimental data. The choice of parameters to check the precision is important, because in addition to their significance, they should be measurable. Some of the most important, commonly provided as the results obtained by the model, are considered here. From Welding parameters welding temperature and welding time and were significant as compared to other factors so the validation was done for the above two most important factors weld temperature versus weld time plot. Hence, the FEA similar trend of results with experimental work are obtained which shows the

validation of the finite element simulation which have less cost and wastage of material as compared to experimental work.

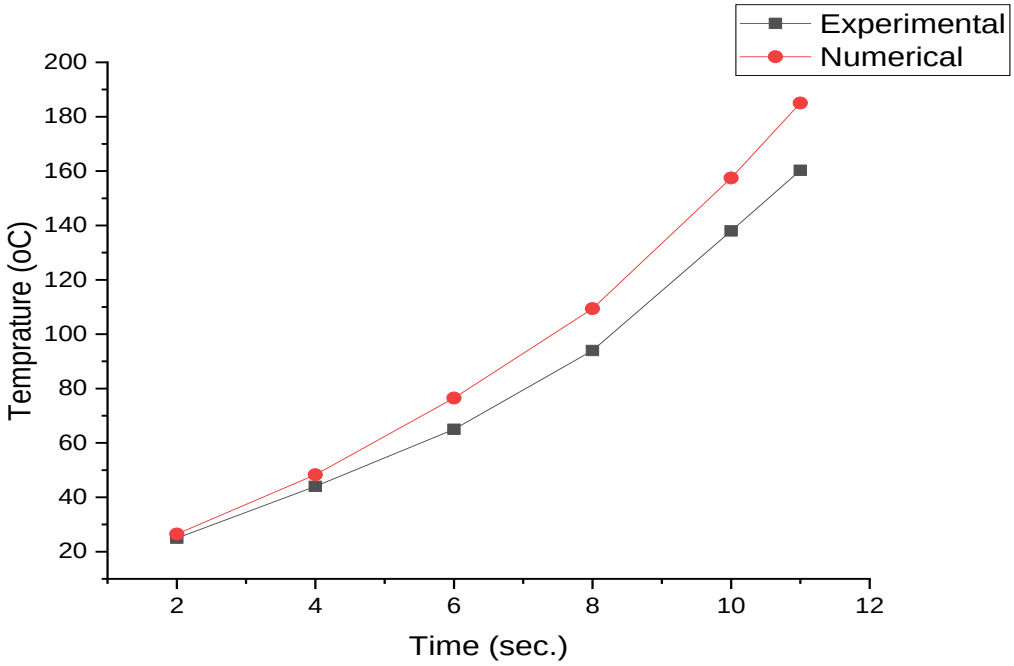

Figure 4.19. Test-1, Weld temperature versus weld time validation plot

As shown in figure 4.19, for both numerical and experimental plot shown temperature is increasing until maximum weld temperature is reached and may be due to weld time limit (11sec.) the temperature will decrease after weld. Hence, the FEA result for those two critical factors weld temperature and weld time the response less agreed with experimental result so validated with 8.40% error, that shows doesn't means that other parameters have no significant agreement but in this case weld temperature have agreed but not strong agreement, that may be due to nature of the material and influence of other welding parameters such as welding current, thickness of weld cover and welding voltage and thickness of weld itself.

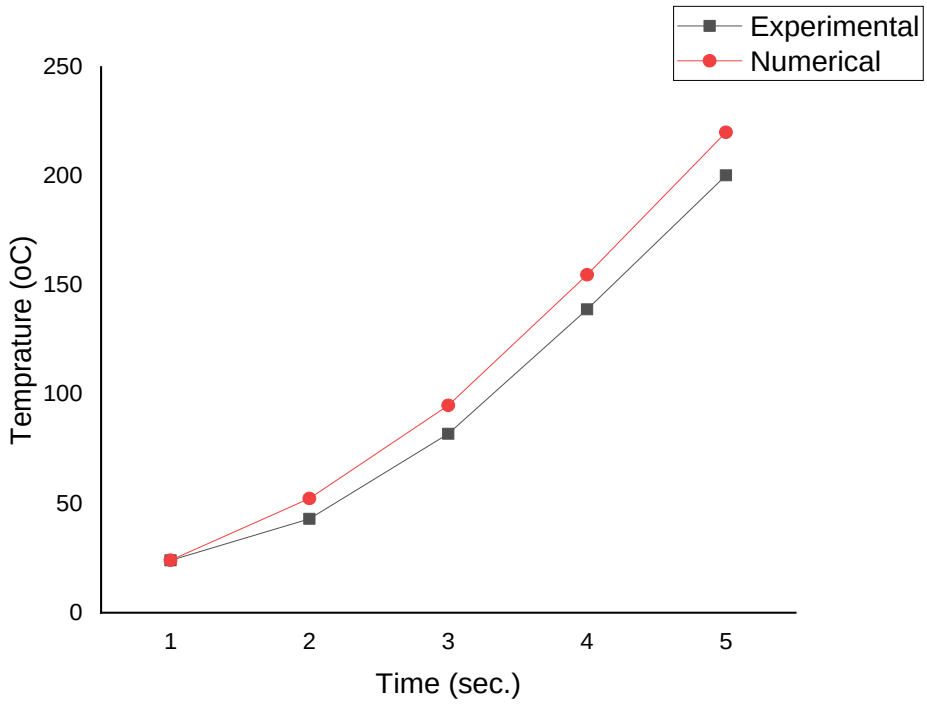

Figure 4.20. Test-2, Weld temperature versus weld time validation plot

As shown in figure 4.20, for both numerical and experimental plot shown temperatures is increasing until maximum weld temperature is reached and may be due to weld time limit (5sec.) the temperature will decrease after weld. Hence, the FEA result for these two critical weld parameters temperature and weld time the response is agreed with experimental result so validated with 8.3% error that shows good agreement but not have strong agreement, that may be due to nature of the material and influence of other welding parameters such as welding current, thickness of weld cover and welding voltage and thickness of weld itself.

.

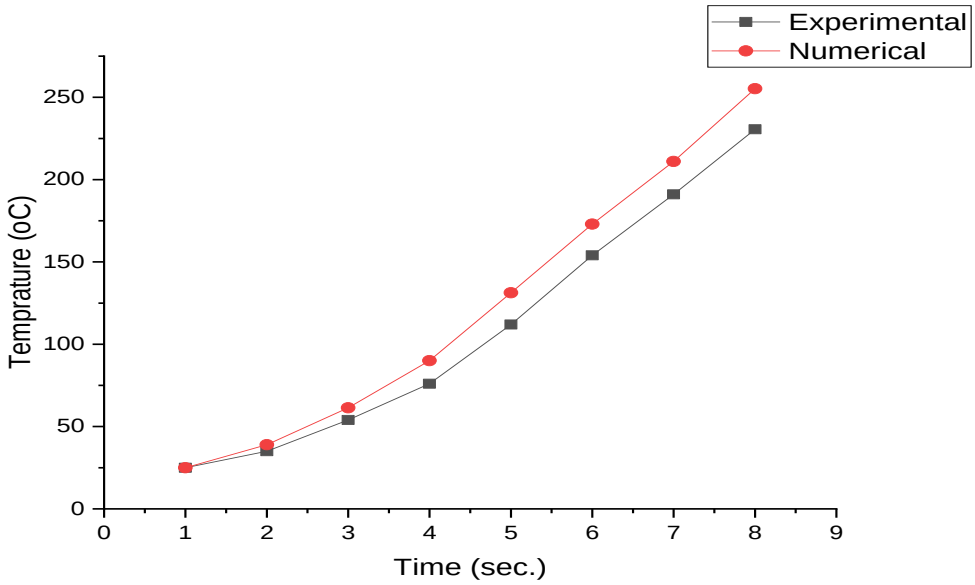

Figure 4.21. Test-3, Weld temperature versus weld time validation plot

As shown in figure 4.21, for both numerical and experimental plot shown temperatures is increasing until maximum weld temperature is reached and due weld time limit (8 sec.) the temperature will decrease after weld. Hence, the FEA result for these two critical weld parameters weld temperature and weld time the response is agreed with experimental result so validated with 10.62% error that show good agreement.

Table 4.2. Summary of temperature response for precision.

No	Experimental Temp Response (^{o}C)	FEA., Max. Temp (^{o}C)	Error (%)
1	160.3	185.01	8.40%
2	200.4	220.14	8.30%
3	230..6	255.26	10.62%

To summarize the effect of weld temperature and weld time by using both experimental and FEA method maximum error recorded while doing with both methods were 20.87% which shows good agreement in between the results but not have strong agreement, that may be due to nature of the material and influence of other welding parameters such as welding current, thickness of weld cover and welding voltage and thickness of weld itself, see table 4.2. Hence, it needs further optimization analysis so that it is clearly discussed in next chapter for the given selected test specimens.

4.5. Parametric Optimization

In this chapter the selected test samples are optimized and S/N ratio, Micro hardness test results are discussed clearly and conclusion, recommendations as well as future working areas are indicated.

Multi-Objective Parametric Optimization

The process parameters for all runs and their level of investigations are tabulated in previous chapter table 4.1. To investigate the degree of importance of the welding process parameters, the ANOVA technique is carried out.

A Minitab program is used to input and analysis the shear strength data. For input variables, encoded units are used. That means the same data in table 4.3 are used in this program.

4.5.1. Main Effect Plot

The main effects plot shows that all the factors appear to be having an effect upon the response variable shear force. This method is used to study the effect of each welding parameter separately and its impact on the shear force, it was obtained the following results, figure 4.22.

The following table 4.3, represents the ranges of spot-welding machine parameters that increase the spot shear force for each thickness: -

Table 4.3. Taguchi Method for Welding Machine Parameters

No	Thickness of Al (mm)	Thickness of Al (mm)	Welding time(sec)
1	0.7	0.6	5
2	1.0	0.8	8
3	1.3	1.0	11

4.5.2. Signal to Noise Ratio

The ‘‘larger is better” S/N characteristics are considered for the sheet metal deformation and given by (Eq. 3). The ANOVA technique is also performed to establish the likely relationship that exists between those factors and the output values.

The deformation is influenced by parameters, the thickness of the substrate, traverse speed, and number of passes usually indicated by the ANOVA. This method is also used to investigate which bending parameters are affecting the response and its effective contribution. The individual contribution of the process parameters affecting the most and least affecting can be calculated by ANOVA.

$$S/N = -10\ log\ 1/n\ \Sigma\ 1/y^2 \qquad \text{(Eq. 3)}$$

Where; y^2 is a variance of y and n is the number of observations.

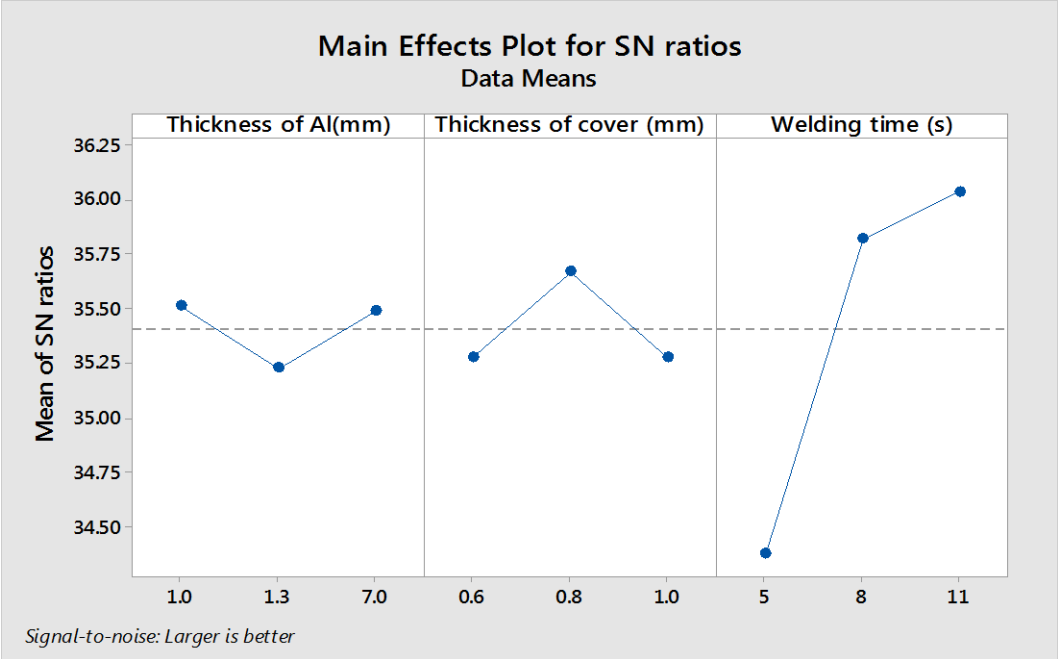

Figure 4.22. Main effects for S/N ratio

The above figure 4.22, shows the main effect plot for S/N ratios for three process parameters, i.e. thickness of aluminum, thickness of mild steel sheet, and welding time. The graphs obtained through the Taguchi technique show that the S/N ratio is highest for parameter welding time.

It is also seen that S/N is lower for the parameter thickness of cover mild steel sheet. So, this can be used to conclude the nature of the effects of different factors. Having from those three parameters, the welding time has a positive effect on the maximum temperature of the nugget area and strength of welded area as it as a direct relationship while the thickness of the aluminum and the thickness of cover mild steel has a low effect on the resulting peak values because the increase in both parameters will reduce the resulting temperature gradient and strength of welded area. It is also important that the cover mild steel has a very low effect when compared to the other two parameters.

Table 4.4. Analysis of Variance for Tensile strength (MPa)

Source	DF	Seq. SS	Contribution	Adj. SS	Adj. MS	F-Value	P-Value
Thickness of Aluminum (mm)	2	271958	3.89%	271958	135979	0.46	0.685
Thickness of cover (mm)	2	227341	3.25%	227341	113670	0.38	0.722
Welding time (s)	2	5894583	84.39%	5894583	2947291	9.97	0.091
Error	2	591367	8.47%	591367	295683		
Total	8	6985247	100.00%				

Where, DF is a degree of freedom, SS is a sequential sum, and MS is mean square sum. The SS, MS, F, P, and percentage contributions calculated for the parameters in the case of maximum tensile strength value are illustrated in table 4.4.

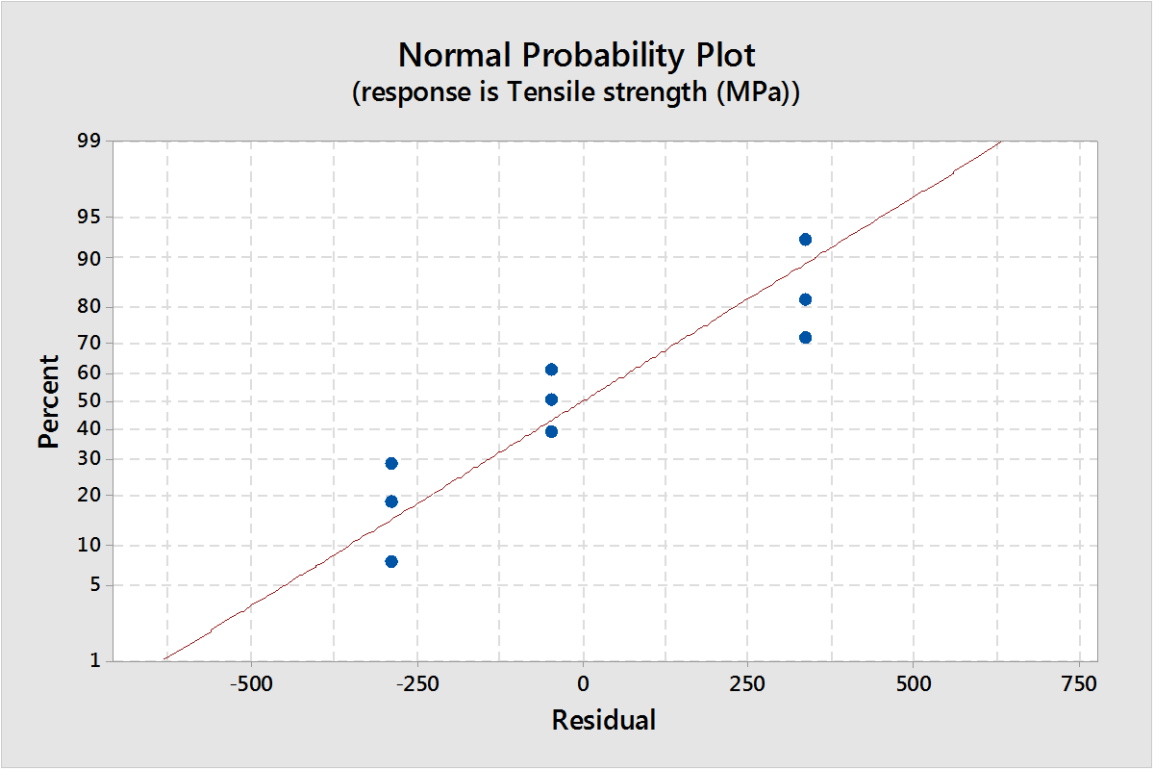

Figure 4.23. Normal probability plot on tensile strength response.

The confidence interval for this analysis is chosen to be 84.39%. So, if the values of P are less than 5%, it implies that the effect of the respective factors will be more significant. Percentage contributions of the thickness of aluminum, thickness of cover sheet, and a welding time are 3.89%, 3.25%, and 84.39%respectively. Based on this analysis, it is found that the degree of importance of

process parameters in attaining the tensile strength of weld joint greatly depends on the welding time, see table 4.4.

4.6. Interaction Plot of Hardness

The percentage of contributions calculated for each process parameters in the case of hardness are also tabulated in 4.5.

Table 4.5.Analysis of Variance for hardness (HRH)

Source	DF	Seq SS	Contribution	Adj SS	Adj MS	F-Value	P-Value
Thickness of Al (mm)	2	0.000004	1.17%	0.000004	0.000002	0.13	0.887
Thickness of cover (mm)	2	0.000027	8.73%	0.000027	0.000013	0.95	0.514
Welding time (s)	2	0.000249	80.88%	0.000249	0.000125	8.77	0.102
Error	2	0.000028	9.22%	0.000028	0.000014		
Total	8	0.000308	100.00%				

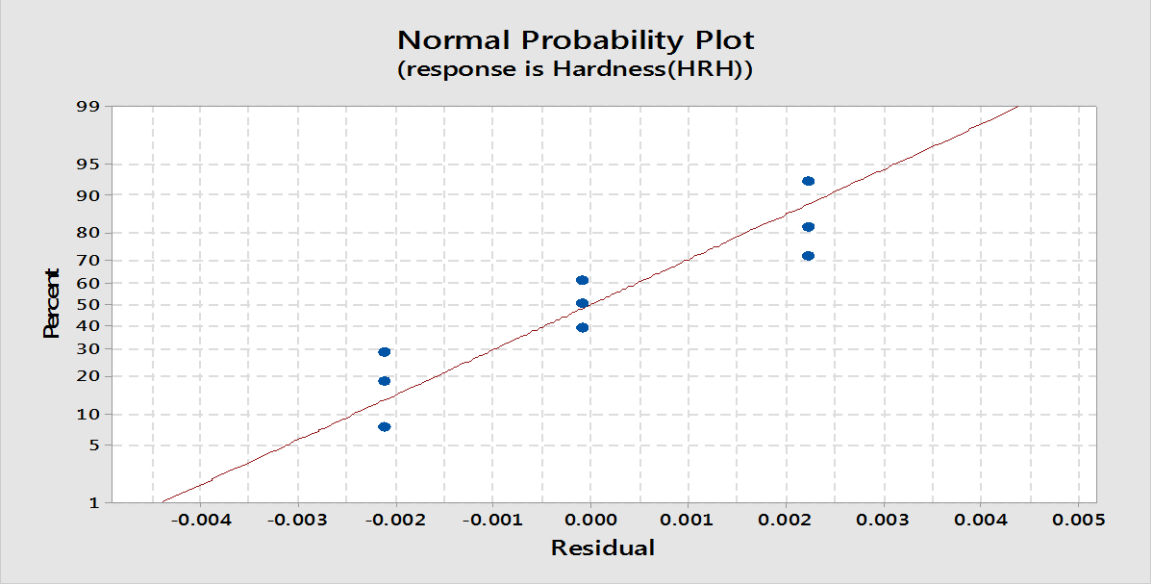

Figure 4.24. Normal probability response on Hardness

In the case of deformation, the percentage of contributions of the thickness of aluminum, thickness of cover sheet, and welding time is 1.17%, 8.73%, and 80.88%respectively. Based on these, it is found that the degree of importance of process parameters in hardness depends on thickness of aluminum, thickness of cover sheet, and welding time. A welding time have the most significant factor, see table 4.5.

The percentage of contributions calculated for each process parameters in the case of hardness are also tabulated in table 4.6.

Table 4.6. Analysis of Variance for Variance for temperature (^{O}c)

Source	DF	Seq. SS	Contribution	Adj. SS	Adj. MS	F-Value	P-Value
Thickness of Aluminum (mm)	2	5519168	9.96%	551916825	275958412	17.41	0.054
Thickness of cover (mm)	2	48676765	87.82%	4867676522	2433838261	153.55	0.006
Welding time (s)	2	91753869	1.66%	91753869	45876934	2.89	0.257
Error	2	31700165	0.57%	31700165	15850082		
Total	8	5543047	100.00%				

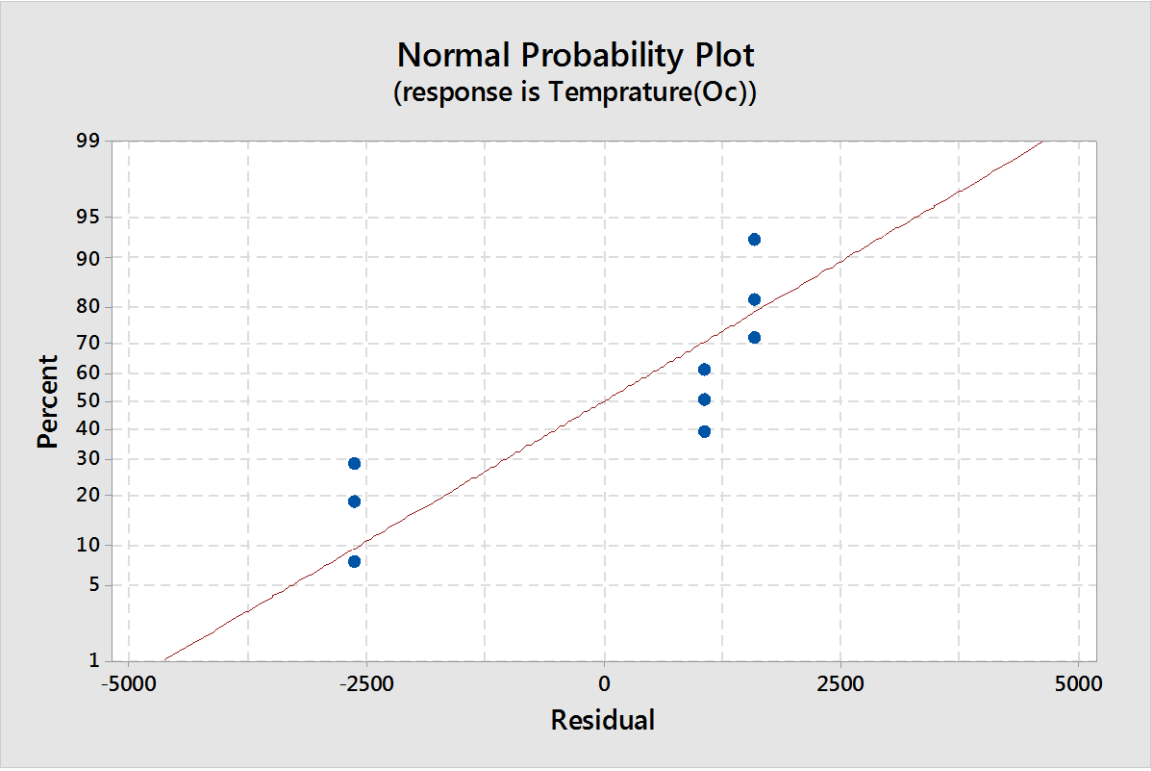

Figure 4.25.Normal Probability of temperature response.

In the case of maximum temperature, the percentage of contributions of the thickness of aluminum, thickness of cover sheet, and welding time is 9.96%, 87.82%, and 1.66% respectively see figure 4.26. Based on these, it is found that the degree of importance of process parameters in maximum

temperature depends on thickness of aluminum, thickness of cover sheet, and welding time. A thickness of cover mild steel sheet has the most significant factor, see table 4.6.

- **Interaction plots for the process parameters with their respective responses.**

Effects of thickness of aluminum, thickness of cover mild steel, and welding time on tensile strength.

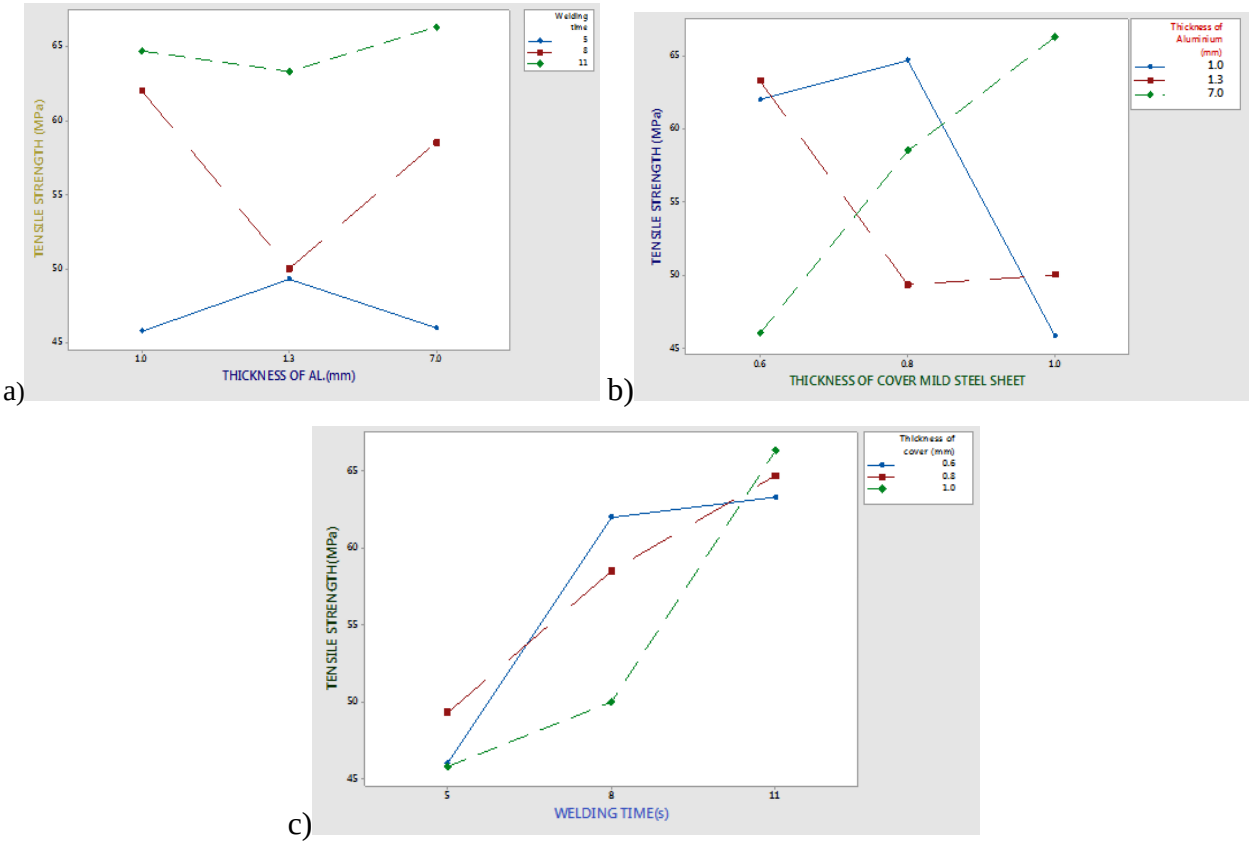

Figure 4.26. The combined effect of the thickness of aluminium (a), thickness cover mild steel sheet (b), and welding time (c) on the tensile strength response.

The above figure 4.26, shows the main effect plot for S/N ratios for three process parameters, i.e. thickness of aluminum, thickness of mild steel sheet, and welding time. The graphs obtained through the Taguchi technique show that the S/N ratio is highest for parameter welding time.

It is also seen that S/N is lower for the parameter thickness of cover mild steel sheet. So, this can be used to conclude the nature of the effects of different factors.

- **Effects of thickness of aluminum, thickness of cover mild steel, and welding time on hardness.**

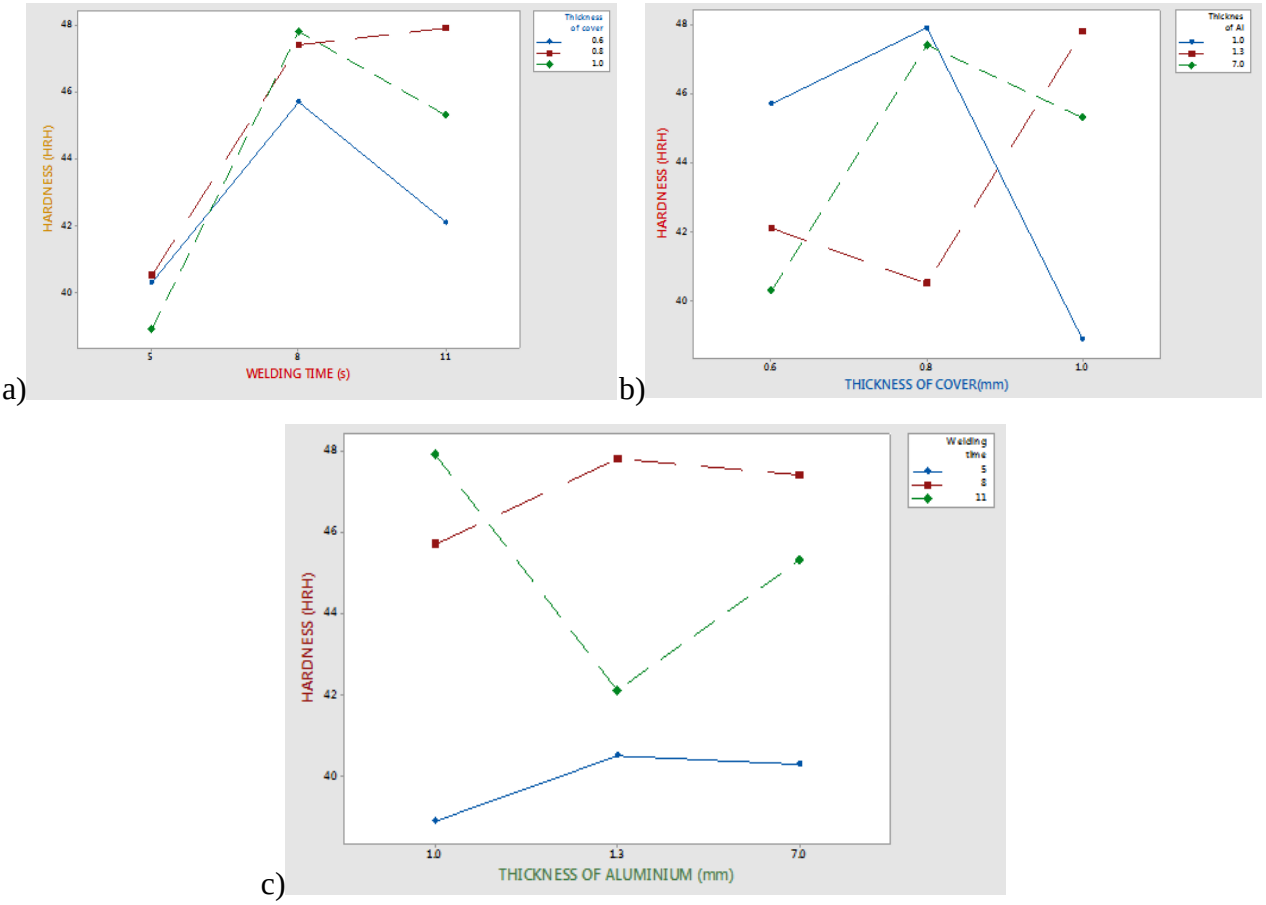

Figure 4.27. The combined effect of the (A) thickness of aluminum, (B) thickness of cover mild steel, and (C) welding time on the hardness response

The above figure 4.27, shows the main effect plot for S/N ratios for three process parameters, i.e. thickness of aluminum, thickness of mild steel sheet, and welding time. The graphs obtained through the Taguchi technique show that the S/N ratio is highest for parameter welding time.

It is also seen that S/N is lower for the parameter thickness of cover mild steel sheet. So, this can be used to conclude the nature of the effects of different factors.

- **Effects of thickness of aluminum, thickness of cover mild steel, and welding time on temperature**

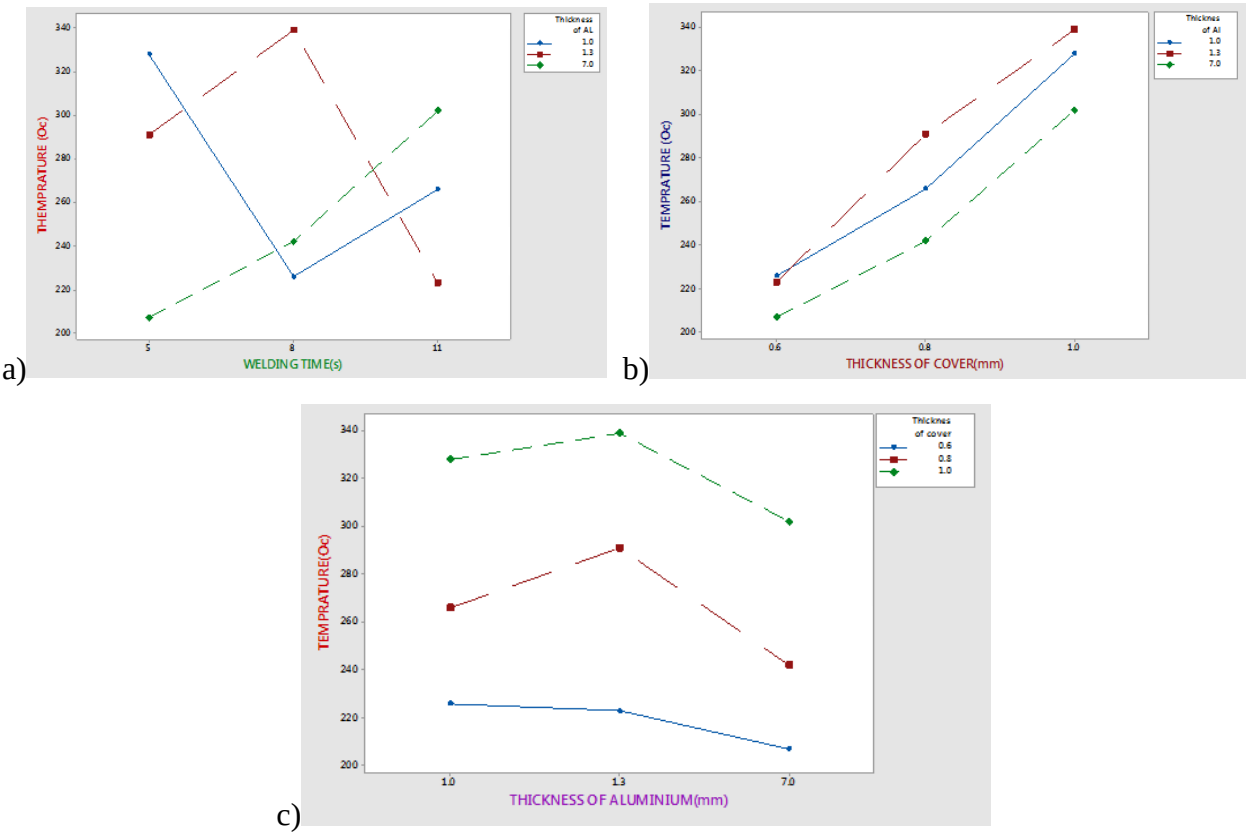

Figure 4.28. The combined effect of the thickness of aluminum (A), thickness of cover mild steel and (B), welding time (C) on the temperature response.

The above figure 4.28, shows the main effect plot for S/N ratios for three process parameters, i.e. thickness of aluminum, thickness of mild steel sheet, and welding time. The graphs obtained through the Taguchi technique show that the S/N ratio is highest for parameter welding time.

It is also seen that S/N is lower for the parameter thickness of cover mild steel sheet. So, this can be used to conclude the nature of the effects of different factors.

The following table 4.7 represents the ranges of spot-welding machine parameters that increase the resistance spot shear force for each thickness.

Table 4.7. Summery on the above tensile and hardness of nine (9) test results

Thickness of Al	Thickness of cover	Welding (T)	Tensile strength	Hardness	SNRA2	MEAN2	RESI	RESI_1	SRES	SRES_1
0.7	0.6	5	46	40.3	32.642	43.15	-288.0	0.002	-1.12	1.25
0.7	0.8	8	58.5	47.4	34.333	52.95	-46.52	-0.002	-0.18	-1.19
0.7	1	11	66.3	45.3	34.468	55.8	334.61	-0.0001	1.305	-0.057
1	0.6	8	62	45.7	34.324	53.85	334.61	-0.0001	1.305	-0.057
1	0.8	11	64.7	47.9	34.719	56.3	-288.0	0.002	-1.12	1.252
1	1	5	45.8	38.9	32.450	42.35	-46.52	-0.002	-0.18	-1.194
1.3	0.6	11	63.3	42.1	33.905	52.7	-46.52	-0.002	-0.18	-1.194
1.3	0.8	5	49.3	40.5	32.919	44.9	334.61	-0.0001	1.305	-0.057
1.3	1	8	50	47.8	33.779	48.9	-288.08	0.002	-1.12	1.252

➢ Regression Analysis for the Process Output.

The fitted equation for the general linear model that describes the relationship between the input and output parameter is given by the following equation. This analysis is usually used to find the relationship between the process parameters and the tensile strength.

Tensile strength (MPa)^2 = 3222 + 89 AT (mm)-0.7+ 154 AT (mm)-1.0- 243 AT (mm)-1.3+ 100 CT (mm)-0.6+ 124 CT (mm)-0.8- 224 CT (mm)-1.0- 1007 W*t* (s)-5+ 33 W*t* (s)-8 + 974 W*t* (s)-11

Where, AT is the thickness of the aluminum sheet in millimeter when it is 0.7mm,1.0mm, and 1.3mm respectively, CT is thickness of the cover mild steel sheet in millimeter, Wt.: - Indicates welding time in second respectively.

Table 4.8. Model summary for tensile strength

S	R-sq.	R-sq.(adj.)	Press	R-sq.(pred.)
543.768	91.53%	66.14%	11975174	0.00%

The R-sq. is a statistical measure that provides information about how close data are to be fitted with a regression line. The R^2 value in this model gives 99.57 % which indicates that this model can be used with sufficient accuracy.

- **Regression Equation**

Hardness (HRH)^-0.5= -0.15111 + 0.00066 Thickness of Aluminum (mm)-0.7
+ 0.00019 Thickness of Al (mm)-1.0
- 0.00085 Thickness of Al (mm)-1.3
- 0.00208 Thickness of cover (mm)-0.6
+ 0.00215 Thickness of cover (mm)-0.8
- 0.00007 Thickness of cover (mm)-1.0 - 0.00722 Welding time (s)-5
+ 0.00517 Welding time (s)-8 + 0.00205 Welding time (s)-11

Table 4.9. Model Summary for Transformed Response

S	R-sq.	R-sq.(adj.)	Press	R-sq.(pred.)
0.0037704	90.78%	63.10%	0.0005758	0.00%

- **Regression Equation**

Temperature (℃)^2= 74596 - 10390 Thickness of Aluminum (mm)-0.7
+ 1876 Thickness of Al (mm)-1.0
+ 8514 Thickness of Al (mm)-1.3 - 26711 Thickness of cover (mm)-0.6
- 3262 Thickness of cover (mm)-0.8 + 29974 Thickness of cover (mm)-1.0+ 3775 Welding time (s)-5 + 258 Welding time (s)-8
- 4033 Welding time (s)-11

Table 4.10. Model Summary for Transformed Response

S	R-sq.	R-sq.(adj.)	Press	R-sq.(pred.)
3981.22	99.43%	97.71%	641928334	88.42%

4.7. Results of Hardness Tests and Microstructure Examinations

To do hardness test and microstructure examination, initially the determination of optimal condition to avoid extra wastage of materials and time the 3-selected test samples are taken as shown table 4.11.

Table 4.11. Determination of optimal factor setting

Factor	Code	Level	Optimum level
Thickness aluminum	A	1	1
Thickness of cover sheet	B	1	0.8
Welding time	C	1	11

The optimal condition is the optimal factor setting which yields the optimum performance. In this case, it is the factor setting which provides the highest tensile strength and the higher hardness at the highest maximum temperature values. So, the optimal condition is obtained by identifying the levels of significant control factors that yield the highest S/N ratio and higher stronger and harder.

The average signal to noise ratio value for the optimum condition is shown in table 4.11. Based on the larger is better characteristics of S/N, a larger value of this yields better results. Accordingly, the 1mm thickness of Aluminum sheet with 0.8mm of cover mild steel sheet and the 11 second of welding time is the best optimum combinations of the parameters which yield the larger value of tensile strength and hardness of the welded area of the aluminum alloy.

To do this experiment the above three optimized samples are selected and tested their micro structure examination and hardness tests are done. After conducting the microstructure test, examination the weld cross-section shows that the microstructure of base metal, HAZ and NZ is various from one region to another. The following results have been obtained,

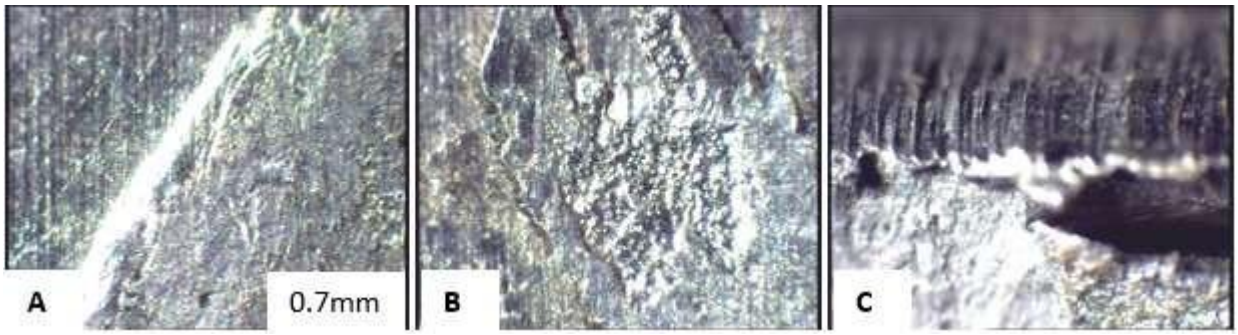

Figure 4.29 Cross section of the 0.7-mm-thick aluminum-clad mild sheet: the thickness of the aluminum layer is 0.6 mm and the thickness of the steel layer is 0.8 mm

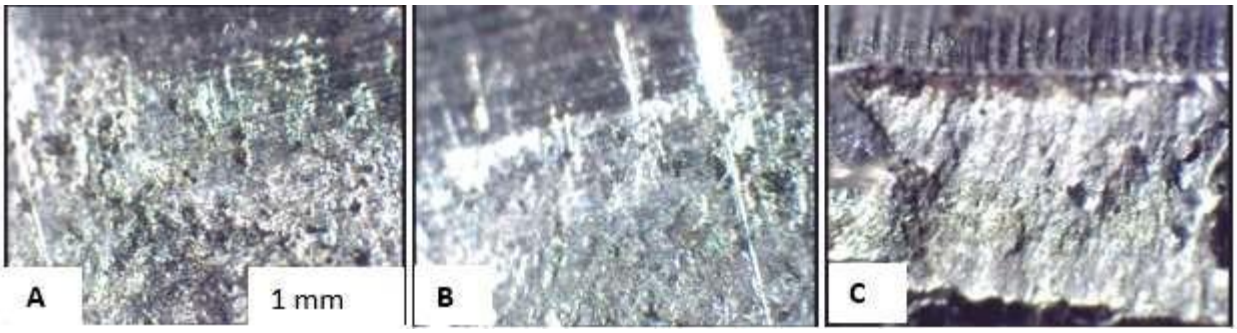

Figure 4.30. Cross section of the 1 mm-thick aluminum-clad mild sheet: the thickness of the aluminum layer is 0.8 mm and the thickness of the steel layer is 0.8 mm.

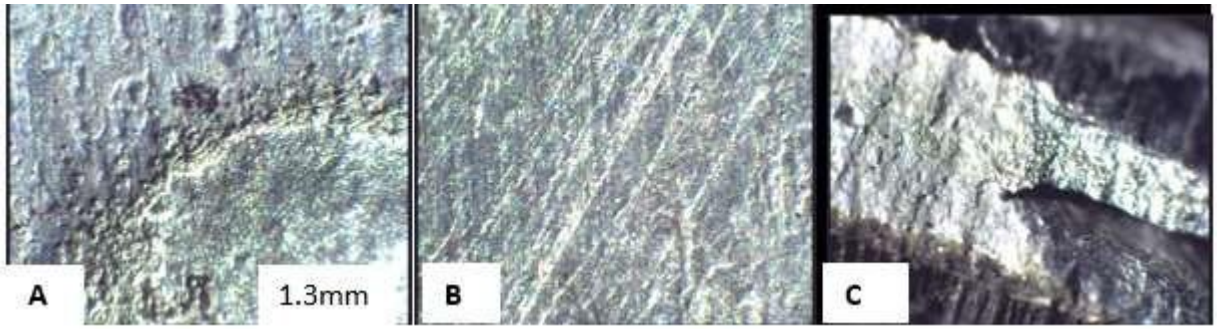

Figure 4.31. Cross section of the 1.3mm-thick aluminum-clad mild sheet: the thickness of the aluminum layer is 1mm and the thickness of the steel layer is 0.8 mm.

Macrostructure Test After conducting the microstructure test, examination the weld cross-section shows that the microstructure of base metal, HAZ and NZ is various from one region to another. The following results have been obtained, Figure (4.29, 4.30 and 4.31). It was observed that the microstructure of AA 2017 in NZ consists of very fine equated grains (smaller size) and uniformly distributed fine precipitates. In general, welding temperature and welding time are the most important factors in controlling heat input for resistance spot welding. Spot weld parameters are the reason for the variation of microstructure. The microstructure of all these spot welds structure is influenced by the degree of cooling (Hussein & Barrak, 2018).

In general, welding current and welding time are the most important factors in controlling heat input for resistance spot welding. Spot weld parameters are the reason for the variation of microstructure. The microstructure of all these spot welds structure is influenced by the degree of cooling.

CHAPTER FIVE

5. Conclusions and Recommendations for Future Study

5.1. Conclusions

The research was primarily focused on to perform Experimental and Finite Element Investigation of Resistance Spot Welding on Aluminum AA 2017. Based on the finding the following conclusions are made on Experimental and Finite Element Investigation of Resistance Spot Welding on Aluminum Al-2017.

- Variation of weld sheet thickness, cover sheet thickness, welding time, with constant welding current and electrode force have strong influence on the weld joint response (welding strength, welding temperature, weld deformation).
- Percentage contributions of the thickness of aluminum, thickness of cover sheet, and a welding time are 3.89%, 3.25%, and 84.39%respectively. Based on this analysis, it is found that the degree of importance of process parameters in attaining the tensile strength of weld joint greatly depends on the welding time.
- In the case of deformation, the percentage of contributions of the thickness of aluminum, thickness of cover sheet, and welding time is 1.17%, 8.73%, and 80.88% respectively. A welding time have the most significant factor.
- In the case of temperature, the percentage of contributions of the thickness of aluminum, thickness of cover sheet, and welding time is 9.96%, 87.82%, and 1.66% respectively. A thickness of cover mild steel sheet has the most significant factor.
- The microstructure of AA 2017 in NZ consists of very fine equated grains (smaller size) and uniformly distributed fine precipitates.
- Welding temperature and welding time are the most important factors in controlling heat input for resistance spot welding. Spot weld parameters are the reason for the variation of microstructure.
- Experimental test result of tension test shows the maximum stress is ranging between (40-100MPa) which is strongly much with FEA result in which the maximum result ranges between (60-100MPa).

- For both experimental and FEA results the maximum von-Misses stress is found on tip of weld electrode and around the weld areas.
- Validated result of two selected most significant factors (weld temperature and weld time) validation on the first three samples shows for FEA and Experimental works shows good agreement, Maximum Error is 10.62% which is good agreement but not strong agreement. May be due to nature of the material and combined effect of other weld parameters.

5.2. Recommendations for Future Works

This research is addressed identified literature gaps which are mentioned on literature section and while doing this thesis work some limitations are not addressed in this thesis so that it this thesis recommends for future further works to do better scientific investigation on resistance spot welding and to put scientific knowledge on effect of weld parameters on about weld area.

- Investigation on effect of electrode tip diameter and geometry on RSW.
- Investigation on effect of variation on welding current on RSW.
- Investigation on effect of different electrode force on RSW.
- Investigation on effect of variation on welding temperature on weld strength and hardness of RSW.
- Study the effect of the weld gap between two spots on RSW.

References

Alden, D. (2017). Modal Analysis of Resistance Spot Welding for Dissimilar Plate Structure.

Alizadeh Sh, M., Pouranvari, M., & Marashi, S. P. H. (2015). Welding metallurgy of stainless steels during resistance spot welding part II – heat affected zone and mechanical performance. *Science and Technology of Welding and Joining*, *20*(6), 512–521. https://doi.org/10.1179/

Brien, A. O. Welding Handbook (Vol. 3), 2000.

Chen, J. Z., & Farson, D. F. (2006). Analytical modeling of heat conduction for small scale resistance spot welding process. *Journal of Materials Processing Technology*, *178*(1–3), 251–258. https://doi.org/10.1016/

Dancette, S., Fabrègue, D., Massardier, V., Merlin, J., Dupuy, T., & Bouzekri, M. (2011). Experimental and modeling investigation of the failure resistance of Advanced High Strength Steels spot welds. *Engineering Fracture Mechanics*, *78*(10), 2259–2272. https://doi.org/10.1016/

Den Uijl, N., Okada, T., Moolevliet, T., Mennes, A., Van Der A, E., Uchihara, M., Smith, S., Nishibata, H., Van Der Veldt, T., & Fukui, K. (2012). Performance of resistance spot-welded joints in advanced high-strength steel in static and dynamic tensile tests. *Welding in the World*, *56*(7–8), 51–63. https://doi.org/

Han, L., Thornton, M., Boomer, D., & Shergold, M. (2010). Effect of aluminium sheet surface conditions on feasibility and quality of resistance spot welding. *Journal of Materials Processing Technology*, *210*(8), 1076–1082. https://doi.org/10.1016/

Hussein, S., & Barrak, O. (2018). Analysis and Optimization of Resistance Spot Welding Parameter of Dissimilar Metals Mild Steel and Aluminum Using Design of Experiment Method Analysis and Optimization of Resistance Spot Welding Parameter of Dissimilar Metals Mild Steel and Aluminum Using. *Eng. &Tech.Journal*, *33*(September), 1999–2011.

Löven born, D. (2016). *3D FE Simulations of Resistance Spot Welding*. 54. http://www.diva-portal.org

Moarref zadeh, A. (2011). Finite-Element Simulation of Resistance Welding Process. Pp31–36.

Naimi, I. K. Al, Saadi, M. H. Al, & Daws, K. M. (2015). *Production & Manufacturing Research: An Open Access Journal Influence of surface pretreatment in resistance spot welding of aluminum AA1050*. *May*, 37–41. https://doi.org/10.1080/ 21693277.2015.1030795

Raut, M., & Achwal, V. (2014). Optimization of spot-welding process parameters for maximum tensile shear strength. *International Journal of Mechanical Engineering and Robotics Research*, v *3*(4), pp506–517.

Rysul, M., & Shawon, A. (2014). *Investigation in to Physical and Mechanical Properties and Failure Mode of Resistance Spot Welded Dissimilar Metal Joints*. 108. http://lib.buet.ac.bd:8080/xmlui/bitstream/handle/123456789/4015 /Full Thesis.pdf.

Shelly, K., & Sahota, D. (2017). A Review Paper on Resistance Spot Welding of Austenitic Stainless Steel 316. *International Journal of Engineering Trends and Technology*, *47*(7), 424–429. https://doi.org/10.14445/22315381/ ijett-v47p270

Sun, X., & Khaleel, M. A. (2004). Resistance spot welding of aluminum alloy to steel with transition material - Part II: Finite element analyses of nugget growth. *Welding Journal (Miami, Fla)*, *83*(7).

Zhao, D., Wang, Y., Zhang, P., & Liang, D. (2019). Modeling and experimental research on resistance spot welded joints for dual phase steel. *Materials*, *12*(7). https://doi.org/10.3390/ .

A**. Nied,** The finite element modeling of the resistance spot welding process, *Welding Research Supplement* (1984) pp123-132.

C. L. Tsai, O. A. Jammal, J. C. Papritan and D. W. Dickinson, Modeling of resistance spot weld nugget growth, *Welding Research Supplement* (1992) pp47-54.

Wenqi Zhang, Computer simulation of resistance welding process and quality control, Proceedings of 1st international seminar on: advances in resistance welding, Copenhagen, Denmark, Oct. 2000.

American Society for Testing and Materials (ASTM), "Standard Test Method for Vickers Hardness of Metallic Metals", ASTM E92-82, Annual book of ASTM standards, vol. 03.01, 2003

Mc Cune, R. W., Armstrong C. G., and Robinson, D. J., "Mixed-Dimensional Coupling in Finite Element Models," International Journal for Numerical Methods in Engineering, 49(6), 725–750, 2000.

Shim K. W., Monaghan D. J., and Armstrong C.G., "Mixed dimensional coupling in finite element stress analysis," Engineering with Computers, 18, 241–252, 2002.

O.P Gupta and Amitava De, An improved numerical modeling for resistance spot welding process and its experimental verification, Journal of Manufacturing Science, Vol 120, pp 246-251, 1998.

H.A Nied, Finite element modeling of a resistance spot welding process, Welding Journal, Vol.63, No.4, pp123-132,1984.

B. Joo, H. Byun and B. Lee, Performance evaluation for the methods of spot weld modeling considering durability, Transactions of the Korean Society of Mechanical Engineers, 29 (2005) 1153-1160.

O. Andersson, Process planning of resistance spot welding, KTH Industrial Engineering and Management (2013).

Y. B. Li, X. M. Lai and G. L. Chen, The influence of interfacial thermal contact conductance on resistance spot weld nugget formation, Advanced Materials Research, 97-101 (2010) 3239-3242.

H. Zhigang, I.-S. Kim, W. Yuanxun, L. Chunzhi and C. Chuanyao, Finite element analysis for the mechanical features of resistance spot welding process, Journal of Materials Processing Technology, 185 (2007) 160-165.

J. Saleem, A. Majid, K. Bertilsson, T. Carlberg and N. U. Islam, Nugget formation during resistance spot welding using finite element model, International Science Index, Mechanical and Mechatronics Engineering, 6 (2012) 1228-1233.

K. Kim, Analysis and application of spot welding process by finite element method, Chung Ang University (2000).

H. Zhigang, W. Yuanxun, L. Chunzhi and C. Chuanyao, A multi-coupled finite element analysis of resistance spot welding process, *Acta Mechanica Solida Sinica*, 19 (2006) 86-94.

Jana Novakova, Lenka Petrkovska, Josef Brychta, Robert Cep, and Lenka Ocenasova, Influence of High Speed Parameters on the Quality of Machined Surface, International Journal of Mechanical, Aerospace, Industrial, Mechatronic and Manufacturing Engineering, Volume 3, Issue 8, 2009, pp-908-911.

Vikas Pare1, Geeta Agnihotri, C.M. Krishna, Optimization Of Machining Parameters In High Speed End Milling Of Al-Sic Using Gravitational Search Algorithm. International Journal of Recent Advances in Mechanical Engineering (Ijmech), Volume 2, Issue 4, November 2013, pp.45-51.

D. Gery , H. Long, P. Maropoulos, Effects of welding speed, energy input and heat source distribution on temperature variations in butt joint welding, Journal of Materials Processing Technology 167 (2005) 393–401

Appendix

Table (A):-Experimental study spot weld volt meter response captured

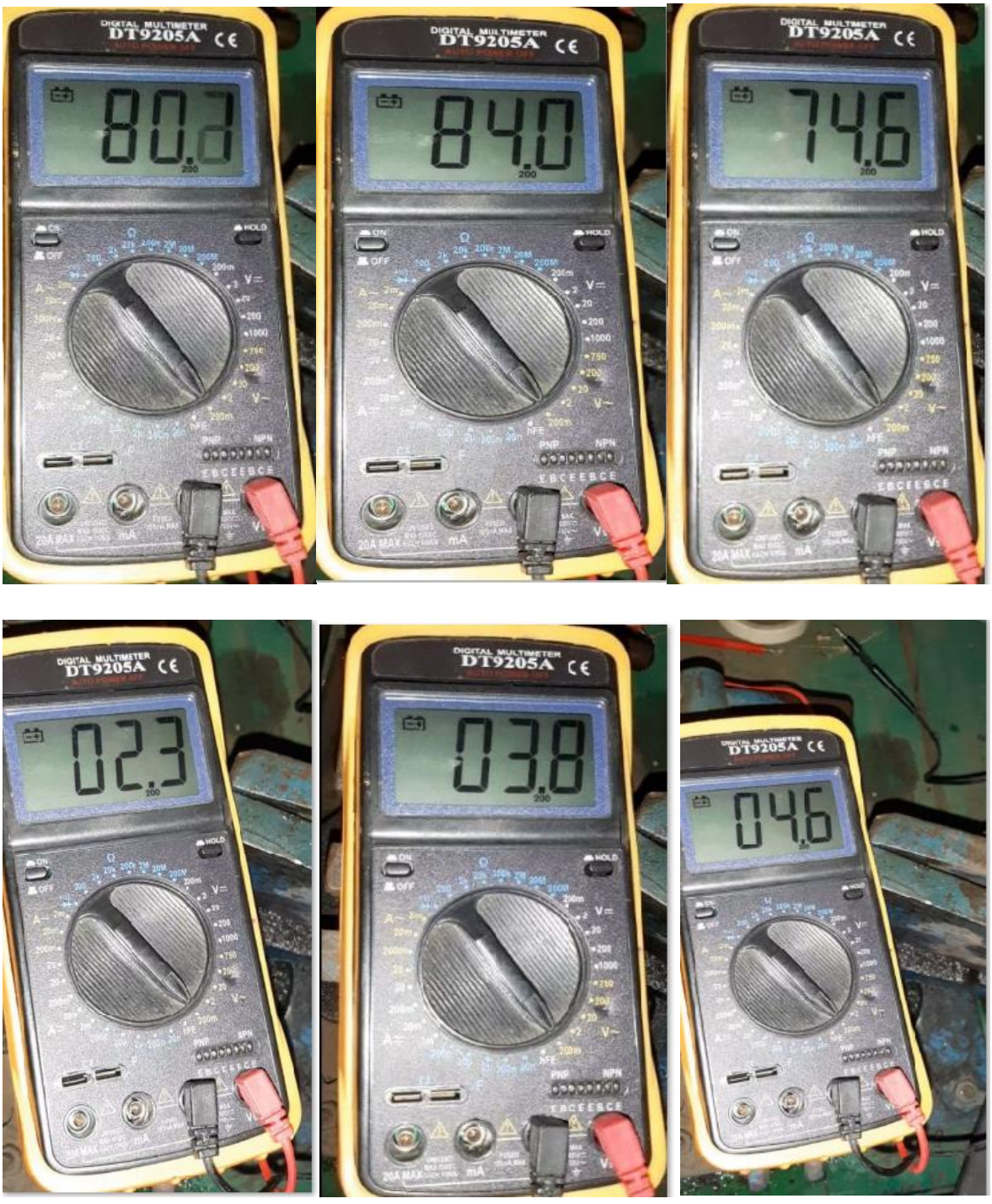


DIGITAL MULTIMETER
DT9205A
36.0


DIGITAL MULTIMETER
DT9205A
31.4


DIGITAL MULTIMETER
DT9205A
46.5


16.1


DIGITAL MULTIMETER
DT9205A
13.2


DIGITAL MULTIMETER
DT9205A
05.2

Table (B): - Welding Machine Details

Type	Hand Held Resistance Spot Welding Machine
Transformer Capacity	3 KVA
Electrode Force (max)	3 KN
Water Flow Rate	2 litter / min
Cooling	Air
Welding Capacity (sheet metal)	0.5-1.5 mm
Welding current (max	3000(A)
Phase	Single phase
Throat depth	100mm
Frequency	50Hz +/- 3%

Table (D): - Temperature readings from the standard thermocouple table.

N

ITS-90 Table for Type N Thermocouple (Ref Junction 0°C) http://reotemp.com

°C	0	1	2	3	4	5	6	7	8	9	10
					Thermoelectric Voltage in mV						
0	0.000	0.026	0.052	0.078	0.104	0.130	0.156	0.182	0.208	0.235	0.261
10	0.261	0.287	0.313	0.340	0.366	0.393	0.419	0.446	0.472	0.499	0.525
20	0.525	0.552	0.578	0.605	0.632	0.659	0.685	0.712	0.739	0.766	0.793
30	0.793	0.820	0.847	0.874	0.901	0.928	0.955	0.983	1.010	1.037	1.065
40	1.065	1.092	1.119	1.147	1.174	1.202	1.229	1.257	1.284	1.312	1.340
50	1.340	1.368	1.395	1.423	1.451	1.479	1.507	1.535	1.563	1.591	1.619
60	1.619	1.647	1.675	1.703	1.732	1.760	1.788	1.817	1.845	1.873	1.902
70	1.902	1.930	1.959	1.988	2.016	2.045	2.074	2.102	2.131	2.160	2.189
80	2.189	2.218	2.247	2.276	2.305	2.334	2.363	2.392	2.421	2.450	2.480
90	2.480	2.509	2.538	2.568	2.597	2.626	2.656	2.685	2.715	2.744	2.774
100	2.774	2.804	2.833	2.863	2.893	2.923	2.953	2.983	3.012	3.042	3.072
110	3.072	3.102	3.133	3.163	3.193	3.223	3.253	3.283	3.314	3.344	3.374
120	3.374	3.405	3.435	3.466	3.496	3.527	3.557	3.588	3.619	3.649	3.680
130	3.680	3.711	3.742	3.772	3.803	3.834	3.865	3.896	3.927	3.958	3.989
140	3.989	4.020	4.051	4.083	4.114	4.145	4.176	4.208	4.239	4.270	4.302
150	4.302	4.333	4.365	4.396	4.428	4.459	4.491	4.523	4.554	4.586	4.618
160	4.618	4.650	4.681	4.713	4.745	4.777	4.809	4.841	4.873	4.905	4.937
170	4.937	4.969	5.001	5.033	5.066	5.098	5.130	5.162	5.195	5.227	5.259
180	5.259	5.292	5.324	5.357	5.389	5.422	5.454	5.487	5.520	5.552	5.585
190	5.585	5.618	5.650	5.683	5.716	5.749	5.782	5.815	5.847	5.880	5.913
200	5.913	5.946	5.979	6.013	6.046	6.079	6.112	6.145	6.178	6.211	6.245
210	6.245	6.278	6.311	6.345	6.378	6.411	6.445	6.478	6.512	6.545	6.579
220	6.579	6.612	6.646	6.680	6.713	6.747	6.781	6.814	6.848	6.882	6.916
230	6.916	6.949	6.983	7.017	7.051	7.085	7.119	7.153	7.187	7.221	7.255
240	7.255	7.289	7.323	7.357	7.392	7.426	7.460	7.494	7.528	7.563	7.597
250	7.597	7.631	7.666	7.700	7.734	7.769	7.803	7.838	7.872	7.907	7.941
260	7.941	7.976	8.010	8.045	8.080	8.114	8.149	8.184	8.218	8.253	8.288
270	8.288	8.323	8.358	8.392	8.427	8.462	8.497	8.532	8.567	8.602	8.637
280	8.637	8.672	8.707	8.742	8.777	8.812	8.847	8.882	8.918	8.953	8.988
290	8.988	9.023	9.058	9.094	9.129	9.164	9.200	9.235	9.270	9.306	9.341
300	9.341	9.377	9.412	9.448	9.483	9.519	9.554	9.590	9.625	9.661	9.696
310	9.696	9.732	9.768	9.803	9.839	9.875	9.910	9.946	9.982	10.018	10.054
320	10.054	10.089	10.125	10.161	10.197	10.233	10.269	10.305	10.341	10.377	10.413
330	10.413	10.449	10.485	10.521	10.557	10.593	10.629	10.665	10.701	10.737	10.774
340	10.774	10.810	10.846	10.882	10.918	10.955	10.991	11.027	11.064	11.100	11.136
350	11.136	11.173	11.209	11.245	11.282	11.318	11.355	11.391	11.428	11.464	11.501
360	11.501	11.537	11.574	11.610	11.647	11.683	11.720	11.757	11.793	11.830	11.867
370	11.867	11.903	11.940	11.977	12.013	12.050	12.087	12.124	12.160	12.197	12.234
380	12.234	12.271	12.308	12.345	12.382	12.418	12.455	12.492	12.529	12.566	12.603
390	12.603	12.640	12.677	12.714	12.751	12.788	12.825	12.862	12.899	12.937	12.974
°C	0	1	2	3	4	5	6	7	8	9	10